ELECTRONIC SUPPLEMENTARY INFORMATION 1

Fluorescence chemosensing of meldonium using a cross-reactive sensor array

Ergin Yalcin[a], Cem Erkmen[b], Tugba Taskin-Tok[c-d], Mehmet Gokhan Caglayan[b]*

[a] Iskenderun Technical University, Faculty of Engineering and Natural Sciences, Engineering Basic Sciences, Hatay, Turkey
[b] Ankara University, Faculty of Pharmacy, Department of Analytical Chemistry, Ankara, Turkey
[c] Gaziantep University, Faculty of Arts and Sciences, Department of Chemistry, Gaziantep, Turkey
[d] Gaziantep University, Institute of Health Sciences, Department of Bioinformatics and Computational Biology, Gaziantep, Turkey
E-mail: gcaglayan@ankara.edu.tr

Table of Contents

Materials and Instruments

All chemicals were purchased from commercial sources and all of them are analytical grade. Meldonium was purchased from ABCR (Karlsruhe, Germany) and reference standard material of meldonium was obtained from Turkish Doping Control Center. Methanol-d4 and Acetonitrile-d3 were obtained from Merck (Darmstadt, Germany). Whatman Chromatography Paper No.1 and all other reagents and materials were purchased from Sigma Aldrich (Steinheim, Germany).

The progress of the reaction was monitored by thin layer chromatography (TLC) was performed by using Merck silica gel (60 F254) plates (0.25 mm) and visualized under ultraviolet light (UV). The melting points were measured using Electrothermal IA9200 apparatus. FT-IR (ATR) spectra were recorded on Perkin-Elmer Spectrum 100 FT-IR spectrophotometer. 1H and 13C NMR (nuclear magnetic resonance) spectra were measured a Bruker Avance 300 Ultra-Shield in D6-DMSO solvent with TMS as internal standard. Chemical shifts are expressed in δ units (ppm). Coupling constants (J) are given in hertz (Hz). High resolution mass spectra (HRMS) for the characterization were recorded using electron ionization (EI) mass spectrometry (Waters-LCT-Premier-XE-LTOF (TOF-MS) instruments; in m/z (rel. %). Mass spectra were taken on a Waters Micromass ZQ connected with Waters Alliance HPLC, using ESI (+) or ESI (−) method, with C-18 column.

BMG LABTECH ClariostarPlus microplate reader (Offenburg, Germany) was used in fluorescence mapping readings. Agilent Cary Fluorescence Spectrophotometer and Cary 60 UV-Vis Spectrophotometer (California, US) were used in fluorescence and UV-Vis absorbance measurements. Agilent Varian Single Cell Peltier Thermostat was combined above spectrometers for temperature controlling. Bruker Ultraflex Extreme MALDI-TOF/TOFMS and Bruker Ultrashield 300 MHz NMR (Massachusetts, US) were used in mass spectrum of complexes and NMR measurements. High Resolution Mass Spectra (HRMS) for characterizations were obtained from Waters-LCT-Premier-XE-LTOF (Massachusetts, US).

Synthesis and characterization of S1-S4

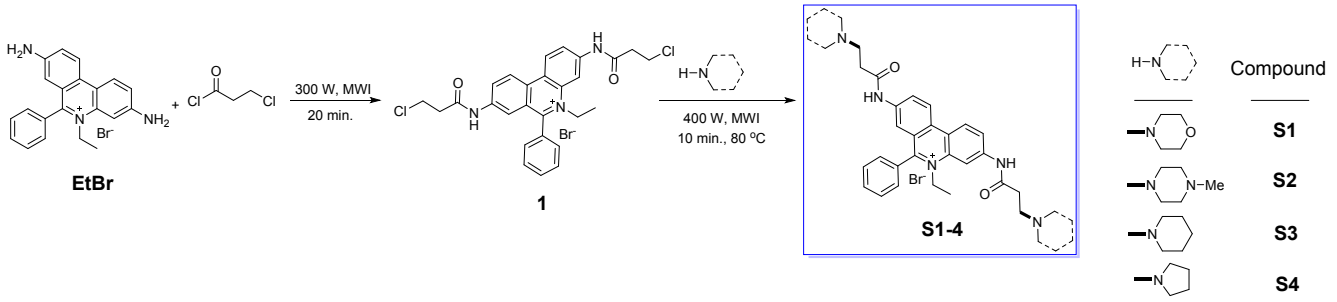

MWI (Microwave irradiation) method for synthesis of intermediate (1)

A solution of ethidium bromide (1.00 mmol, 394 mg), 3-chloropropionyl chloride (2.50 mmol, 240 μL) and a few drops (0.20 mL) of acetonitrile were added in a microwave tube, then stirred 20 min. at 300 W, 70 ºC. After the tube was cooled, the crude was washed with diethyl ether (2 x 15.0 mL) and recrystallized from ethanol-water. (95%, v:v) to give the product (460 mg, 0.80 mmol, 80%) as yellow solid; m.p. 282–284 °C. 1H-NMR (DMSO-d6, 300 MHz) δ (ppm): δ 1.55 (t, 3J = 7.1 Hz, 3H, 5-NCH2CH3), 2.85 (t, 3J = 6.1 Hz, 2H, CH2 adja-cent carbonyl group), 3.03 (t, 3J = 6.1 Hz, 2H, CH2 adjacent carbonyl group), 3.84 (t, 3J = 6.2 Hz, 2H, CH2 adjacent chlorine atom), 3.97 (t, 3J = 6.2 Hz, 2H, CH2 adjacent chlorine atom), 4.65 (q, 3J = 7.1 Hz, 2H, CH2 adjacent to the cationic nitrogen), 7.75-7.90 (m, 6H), 8.00 (d, 4J = 1.8 Hz, 1H), 8.23 (d, 3J = 9.1 Hz, 1H), 8.48 (dd, 3J = 9.1, 4J = 1.8 Hz, 1H),

9.15 - 9.07 (m, 2H), 10.8 (s, 1H, 8-NH), 11.2 (s, 1H, 3-NH); 13C NMR (DMSO-d6, 75 MHz) δ 14.3 (5-NCH2CH3, 50.9 (5-NCH2CH3), 108.3, 119.4, 122.1, 122.6, 124.1, 125.8, 126.2, 128.6, 129.7, 129.8, 130.9, 131.8, 131.7, 134.2, 139.9, 142.1, 163.8 (C6), 169.4 (C=O), 170.0 (C=O); HRMS (EI, CH3CN) found: 494.1401 (C27H26Cl2N3O2) [M-Br]+calcd.: 494.1402.

General MWI (Microwave irradiation) method for synthesis of Chemosensors (S1-4)

Compound 1 (1.00 mmol, 573 mg), alkyl amine (4.00 mmol) and a few drops (0.20 mL) of acetonitrile were added in a microwave reaction vial. The reaction vial was capped, and the mixture was irradiated at 400 W for 10 min. at 80 ^{o}C. After cooling, the crude was washed twice with diethyl ether (2 x 10.0 mL) and recrystallized from the appropriate solvent to yield the products (**S1-4**).

*5-ethyl-6-phenyl-3,8-bis(3-morpholinopropanamido)5-phenanthridinium bromide (**S1**).* Yellow solid. Yield (520 mg, 0.77 mmol, 77 %).m.p. 258-259 ^{o}C (EtOH). ^{1}H-NMR (DMSO-d_6, 300 MHz) δ (ppm): δ 1.52 (t, ^{3}J = 7.2 Hz, 3H, 5-NCH$_2$C$\underline{H}_3$), 2.70-2.30 (m, 16H), 3.53 (t, ^{3}J = 4.3 Hz, 4H, 2 X C$\underline{H}_2$ adjacent to the oxygen atom), 3.58 (t, ^{3}J = 4.3 Hz, 4H, 2 X C$\underline{H}_2$ adjacent to the oxygen atom), 4.64 (q, ^{3}J = 7.2 Hz, 2H, C$\underline{H}_2$ adjacent to the cationic nitrogen), 7.85-7.75 (m, 5H), 7.94 (d, ^{4}J = 1.9 Hz, 1H), 8.20 (d, ^{3}J = 9.4 Hz, 1H), 8.45 (dd, ^{3}J = 9.2, ^{4}J = 1.9 Hz, 1H), 9.20-9.00 (m, 3H), 10.70 (s, 1H, 8-N$\underline{H}$), 11.10 (s, 1H, 3-N$\underline{H}$); ^{13}C NMR (DMSO-d_6, 75 MHz) δ 14.3 (5-NCH$_2$C$\underline{H}_3$), 50.9 (5-NC$\underline{H}_2$CH$_3$), 119.3, 122.0, 122.6, 124.0, 125.7, 126.2, 128.6, 129.8, 130.8, 131.7, 131.9, 134.2, 140.0, 142.3, 163.7, (the peaks of carbonyl carbon atoms could not be observed probably due to the limited solubility of compound; HRMS (EI, CH_3CN) found: 592.3642 ($C_{35}H_{42}N_5O_4$) [M-Br]$^{+}$calcd.: 592.3237.

*5-ethyl-6-phenyl-3,8-bis(4-methylpiperazin-1-yl)propanamido)5-phenanthridinium bromide (**S2**).* Dark yellow solid. (596 mg, 0.85 mmol, 85%) m.p. 245-247 ^{o}C (EtOH). ^{1}H-NMR (DMSO-d_6, 300 MHz) δ (ppm): δ 1.52 (t, ^{3}J = 6.8 Hz, 3H, 5-NCH$_2$C$\underline{H}_3$), 2.00–3.00 (30 H), 4.63 (d, ^{3}J = 6.7 Hz, 2H, C$\underline{H}_2$ adjacent to the cationic nitrogen), 7.85 (m, 5H), 7.95 (d, ^{4}J = 1.7 Hz, 1H), 8.23 (d, ^{3}J = 8.8 Hz, 1H), 8.45 (d, ^{3}J = 8.8 Hz, ^{4}J = 1.5 Hz, 1H), 9.00-9.15 (m, 3H), 10.80 (s, 1H, 8-N$\underline{H}$), 11.20 (s, 1H, 3-N$\underline{H}$); ^{13}C NMR (DMSO-d_6, 75 MHz) δ 14.3 (5-NCH$_2$C$\underline{H}_3$), 34.5 (C$\underline{H}_2$ adjacent carbonyl group), 34.8 (C$\underline{H}_2$ adjacent carbonyl group), 43.4 (NC$\underline{H}_3$ in piperazine ring), 45.6 (2 x NC$\underline{H}_3$ in piperazine rings), 50.9 (5-NC$\underline{H}_2$CH$_3$), 52.2 (C$\underline{H}_2$ at the α-position of nitrogene bonded to alkyl chain), 52.3 (C$\underline{H}_2$ at the α-position of nitrogene bonded to alkyl chain), 53.7, 54.7 (2 x C$\underline{H}_2$ at the α position of nitrogen atom in piperazine ring, 54.8 (2 x C$\underline{H}_2$ at the α position of nitrogen atom in piperazine ring), 108.1, 119.2, 121.9, 122.6, 124.0, 125.7, 126.2, 128.6, 129.8, 130.7, 131.7 131.8, 134.2, 140.0, 142.3, 163.7 (C$\underline{6}$), 171.4 (C$\underline{=}$O), 172.1 (C$\underline{=}$O); HRMS (EI, CH_3CN) found: 622.3875 ($C_{37}H_{48}N_7O_2$) [M-Br]$^{+}$calcd.: 622.3869.

*5-ethyl-6-phenyl-3,8-bis(3-(piperidin-1-yl)propanamido)5-phenanthridinium bromide (**S3**).* Yellow solid. (570 mg, 0.85 mmol 85 %), m.p. 244-245 °C (EtOH). ^{1}H-NMR (DMSO-d_6, 300 MHz) δ (ppm): δ 1.6 - 1.3 (m, 15H), 2.70 - 2.20 (m, 16H), 4.63 (q, ^{3}J = 6.6 Hz, 2H, C$\underline{H}_2$ adjacent to the cationic nitrogen), 7.90 - 7.75 (m, 6H), 8.23 (d, ^{3}J = 8.8 Hz, 1H), 8.49 (d, ^{3}J = 8.8 Hz, 1H), 9.20 - 9.00 (m, 3H), 10.95 (s, 1H, 8-N$\underline{H}$), 11.30 (s, 1H, 3-N$\underline{H}$); ^{13}C NMR (DMSO-d_6, 75 MHz) δ 14.3 (5-NCH$_2$C$\underline{H}_3$), 24.5 (2 x C$\underline{H}_2$ at the γ -position of nitrogene atom in piperidine ring, 26.1 (4 x C$\underline{H}_2$ at the β-position of nitrogen atom in piperidine ring), 34.4 (C$\underline{H}_2$ adjacent carbonyl group), 34.9 (C$\underline{H}_2$ adjacent carbonyl group), 50.9 (5-NC$\underline{H}_2$CH$_3$), 54.0 (2 x C$\underline{H}_2$ at the α-position of nitrogen atom in piperidine ring), 54.2 (at the α-position of nitrogen atom in piperidine ring), 54.6 (C$\underline{H}_2$ at the α-position of nitrogen bonded to alkyl

chain), 54.7 ($\underline{C}H_2$ at the α-position of nitrogene atom bonded to alkyl chain), 108.0, 119.1, 121.9, 122.6, 124.0, 125.6, 126.1, 128.6, 129.8, 130.7, 131.7, 131.9, 134.1, 140.2, 142.5, 163.5 ($\underline{C}$6), 171.7 ($\underline{C}$=O), 172.4 ($\underline{C}$=O); HRMS (EI, CH_3CN) found: 592.3633 ($C_{37}H_{46}N_5O_2$) $[M\text{-}Br]^+$calcd.: 592.3652.

5-ethyl-6-phenyl-3,8-bis(3-(pyrrolidin-1-yl)propanamido)5-phenanthridinium bromide ***(S4).*** Pale yellow solid (514 mg, 0.80 mmol, 80%); m.p. 223–224 °C (dioxane). ^{1}H-NMR (DMSO-d_6, 300 MHz) δ (ppm): δ 1.52 (^{3}J = 6.8 Hz, 3H, 5-$NCH_2C\underline{H}_3$), 1.90-1.60 (m, 8H), 2.85-2.60 (m, 12H), 4.63 (q, ^{3}J = 6.5 Hz, 2H, $C\underline{H}_2$ adjacent to the cationic nitrogen), 7.70-7.85 (m, 5H), 7.98 (s, 1H), 8.25 (d, ^{3}J = 9.00 Hz, 1H), 8.45 (d, ^{3}J = 8.70 Hz, 1H), 9.20 - 9.00 (m, 3H), 10.85 (s, 1H, 8-N$\underline{H}$), 11.30 (s, 1H, 3-N$\underline{H}$); ^{13}C NMR (DMSO-d_6, 75 MHz) δ 14.3 (5-$NCH_2\underline{C}H_3$), 23.5 (2 X $\underline{C}H_2$ at the β position of nitrogen atom in pyrolidine ring, 23.6 (2 x $\underline{C}H_2$ at the β position of nitrogen atom in pyrolidine ring), 50.8 (5-$N\underline{C}H_2CH_3$), 51.6 (4 X $\underline{C}H_2$ at the α-position of nitrogene atom in pyrolidine ring, 53.8 ($\underline{C}H_2$ at the α-position of nitrogene bonded to alkyl chain), 53.9 ($\underline{C}H_2$ at the α -position of nitrogene atom in pyrolidine ring), 108.1, 119.2, 121.9, 122.6, 123.9, 125.6, 126.1, 128.6, 129.8, 130.8, 131.7, 131.9, 134.1, 140.2, 142.5, 163.6 ($\underline{C}$6), (the peaks of carbons on carbonyl groups wasn't observed probably due to the limited solubility of compound; HRMS (EI, CH_3CN) found: 564.3339 ($C_{35}H_{42}N_5O_2$) $[M\text{-}Br]^+$calcd.: 564.3339.

^{1}H NMR and ^{13}C NMR spectra

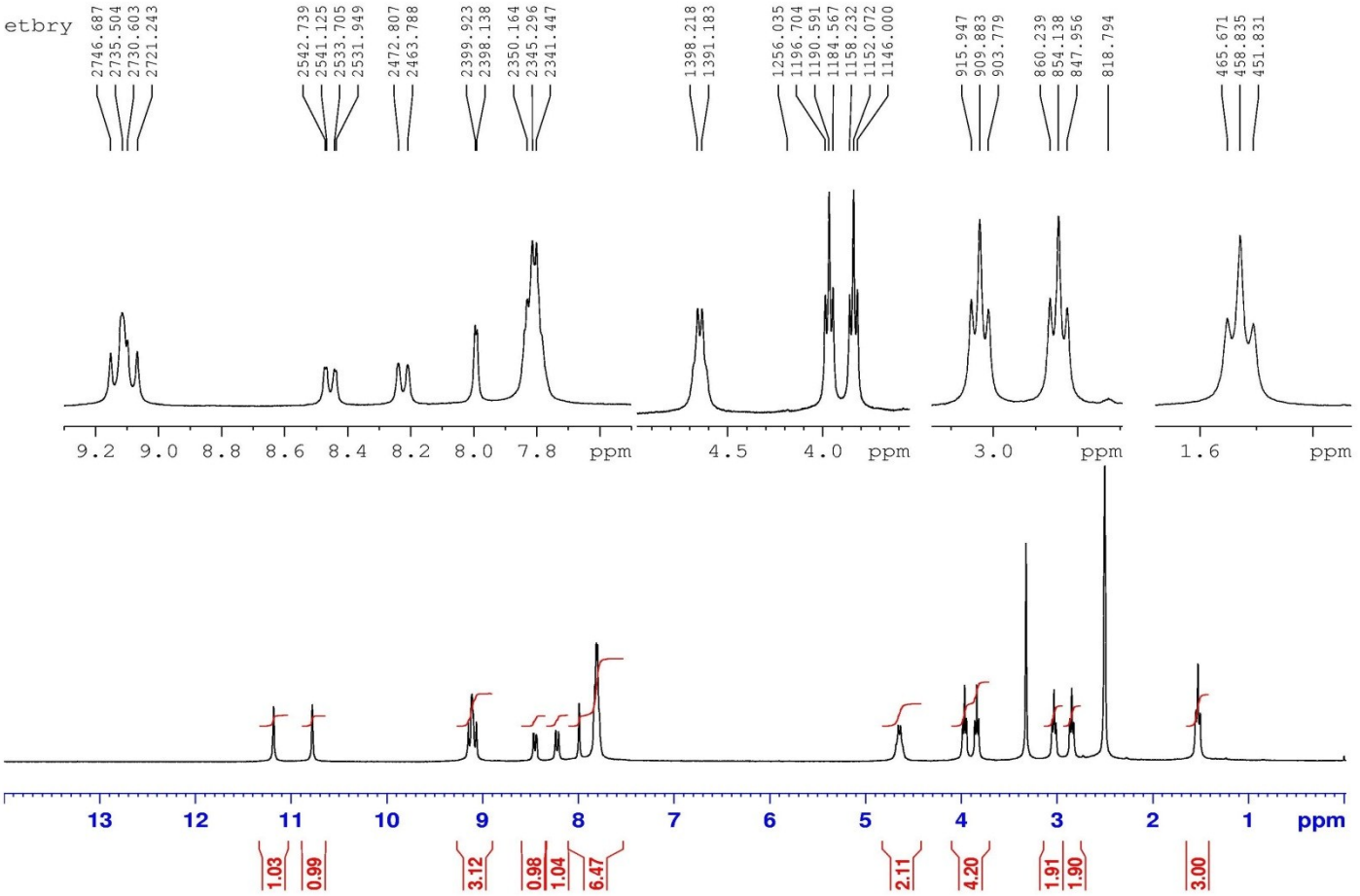

Figure S1: ^{1}H NMR spectrum of compound **1** in DMSO-d_6.

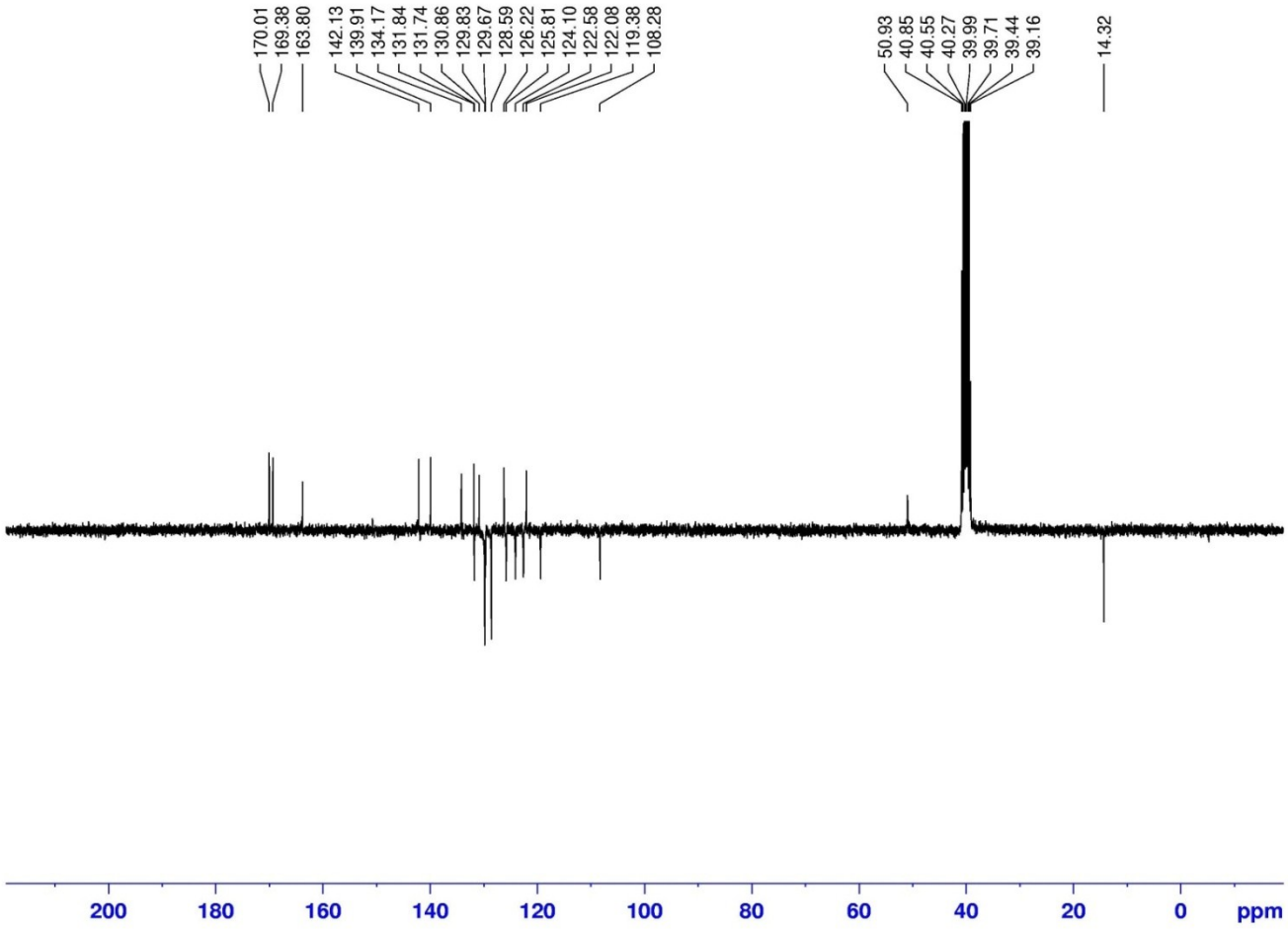

Figure S2: ^{13}C NMR spectrum of compound **1** in DMSO-d_6.

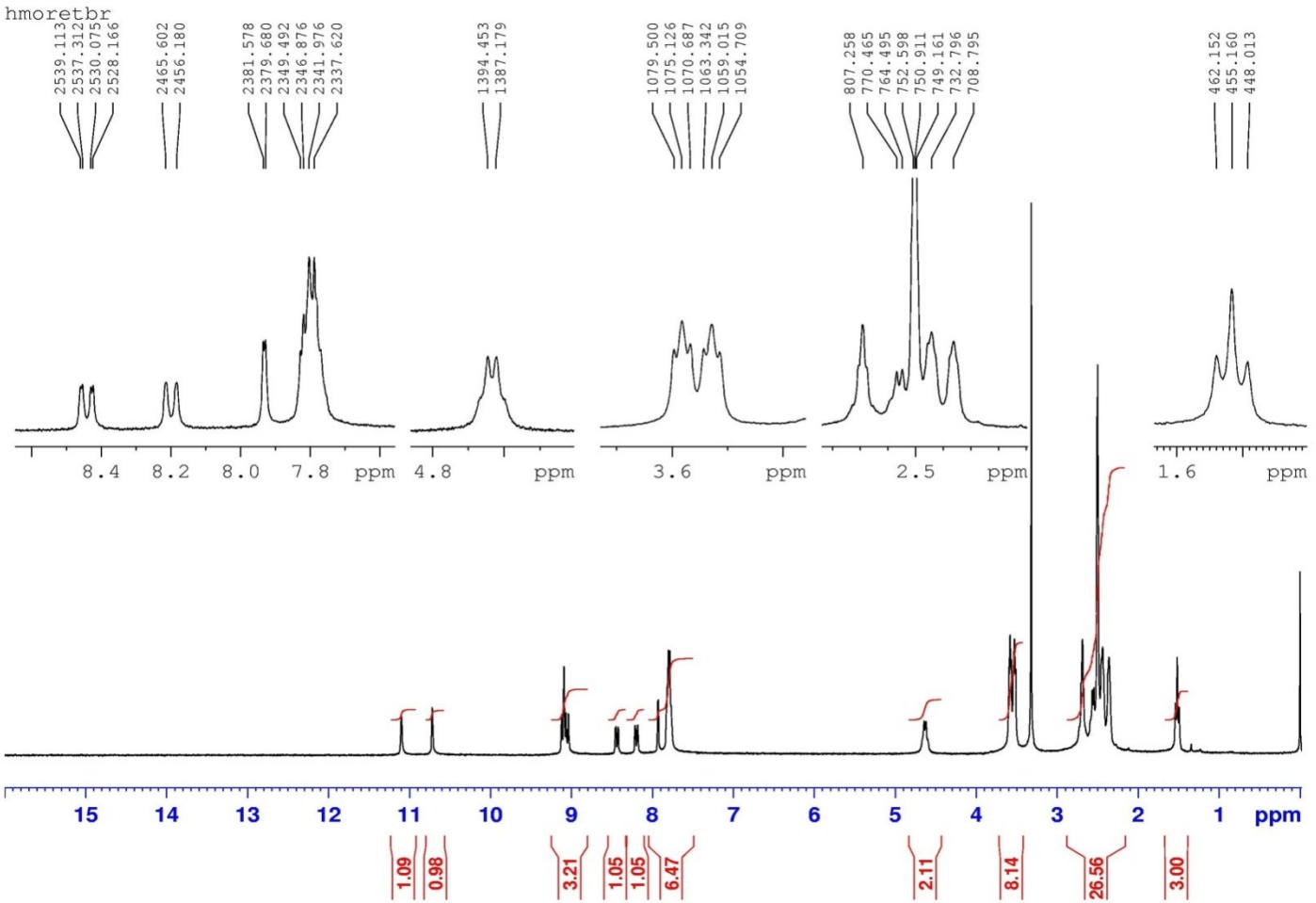

Figure S3: ^{1}H NMR spectrum of compound **S1** in DMSO-d_6.

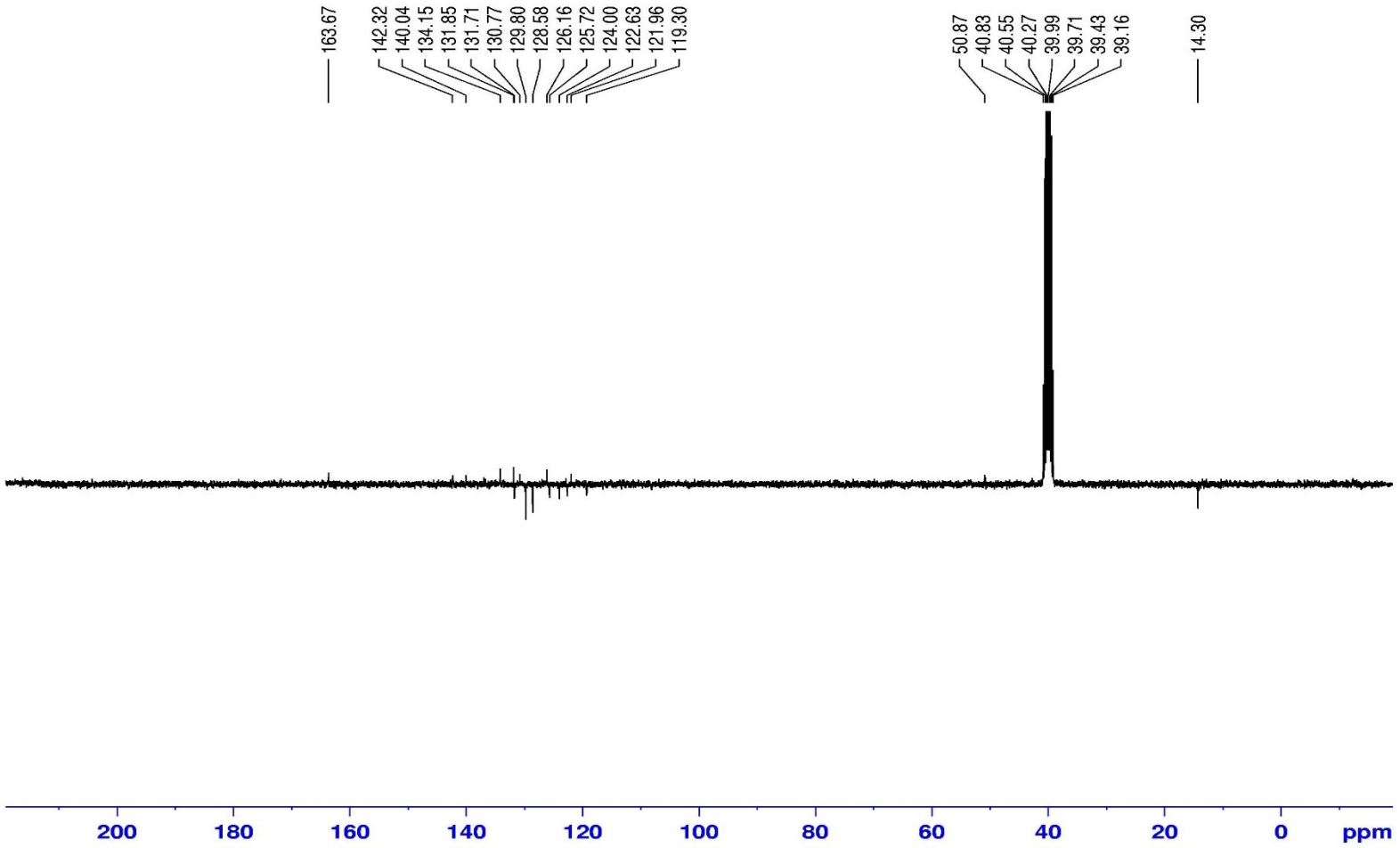

Figure S4: ^{13}C NMR spectrum of compound **S1** in DMSO-d_6.

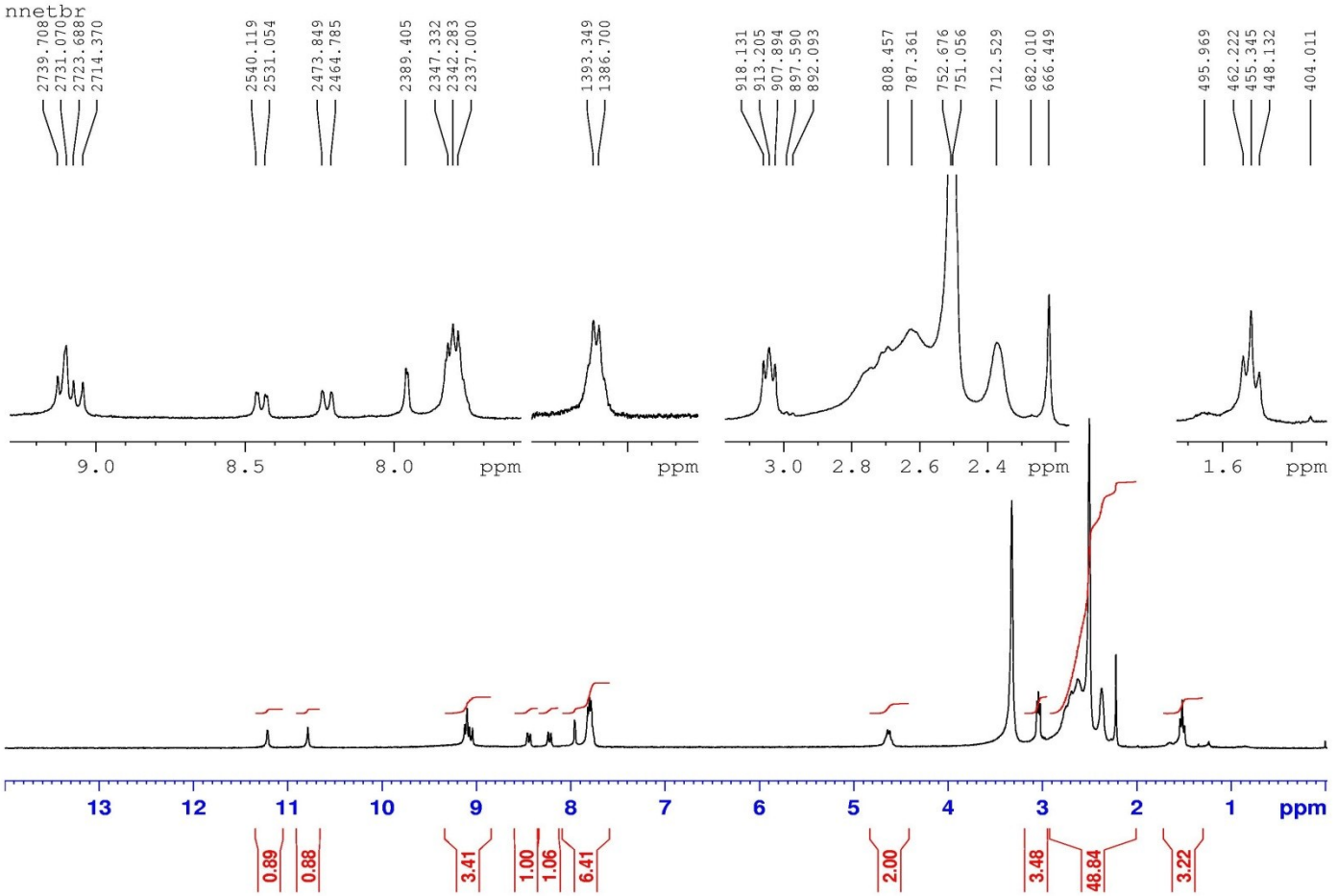

Figure S5: ^{1}H NMR spectrum of compound **S2** in DMSO-d_6.

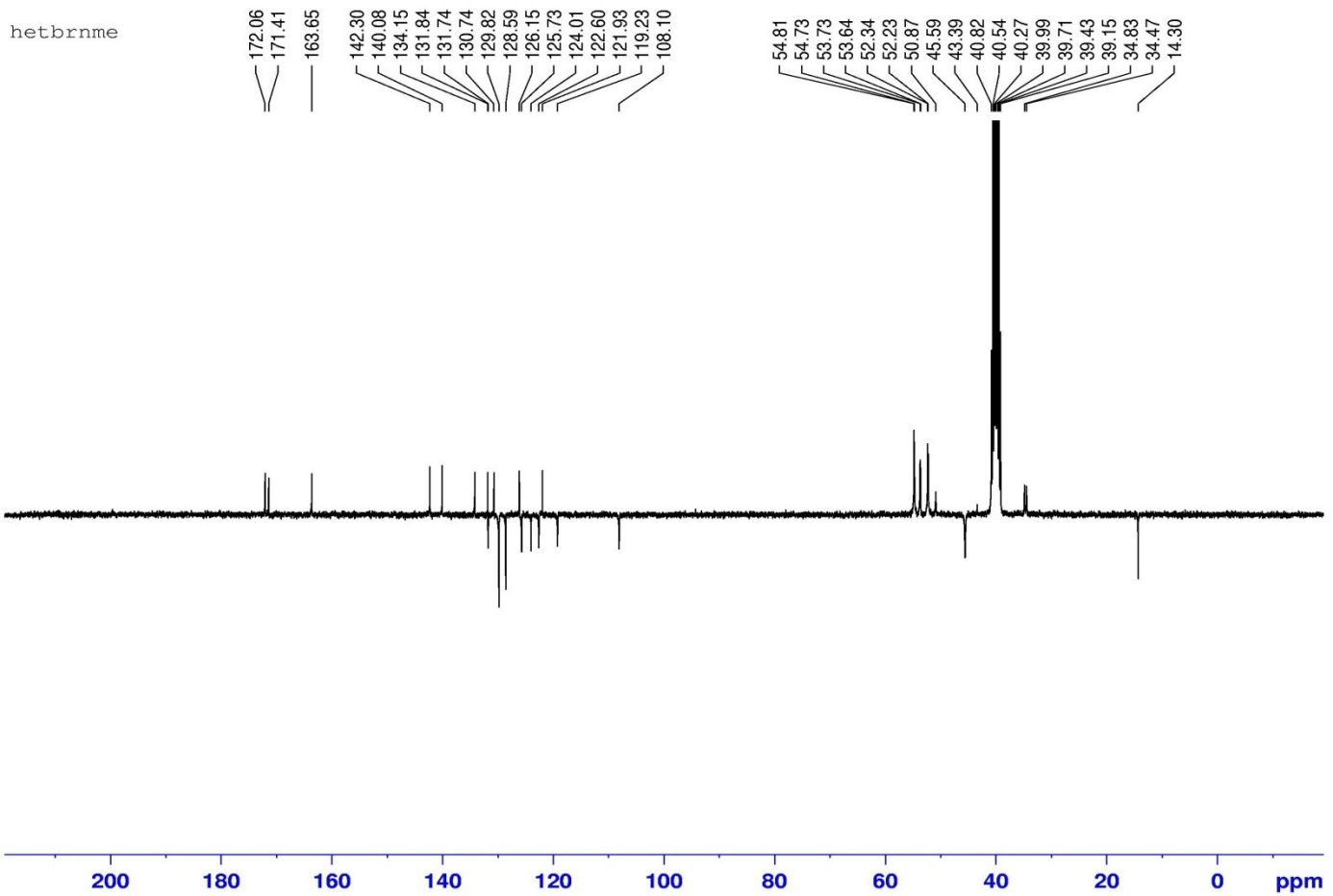

Figure S6: ^{13}C NMR spectrum of compound **S2** in DMSO-d_6.

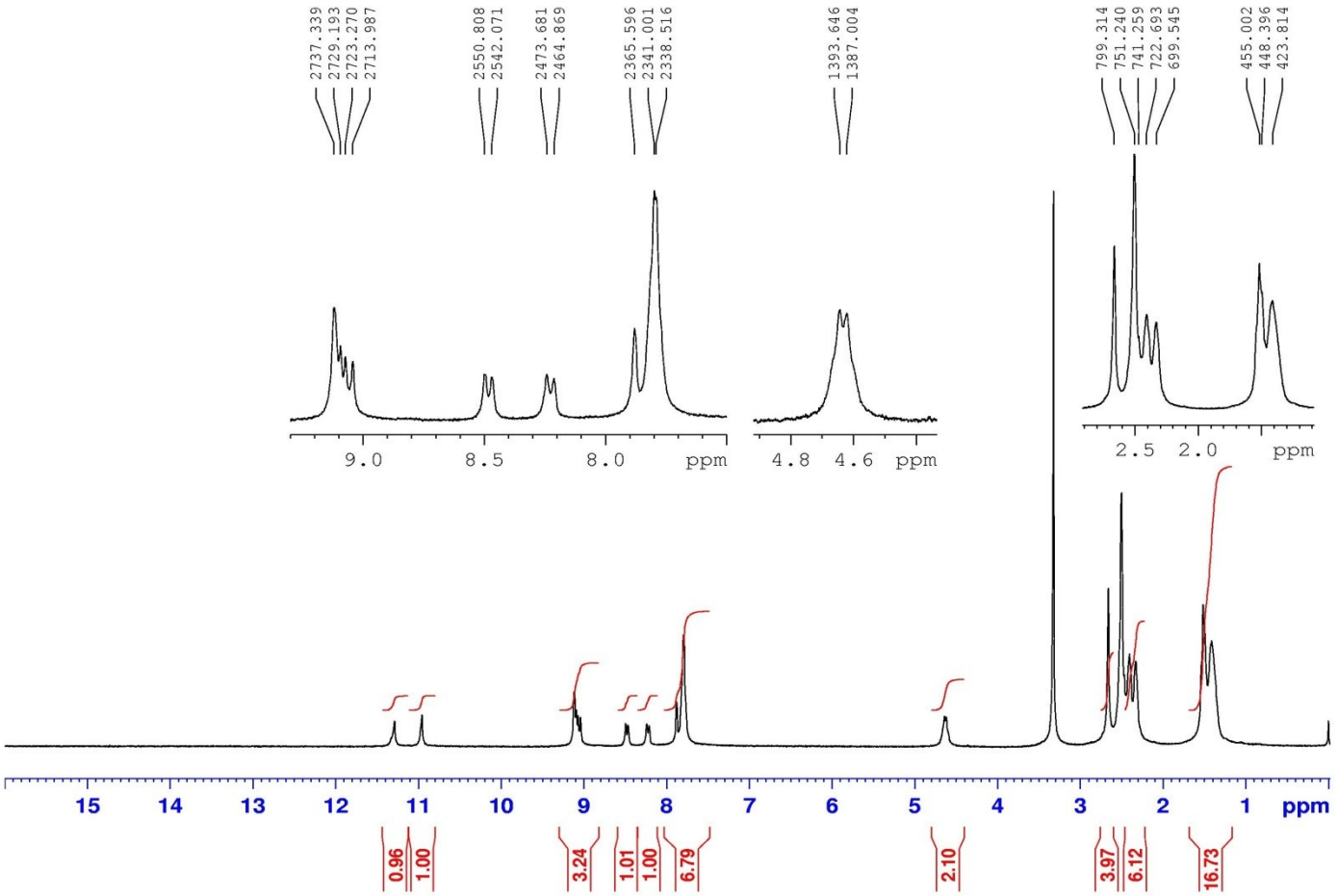

Figure S7: ^{1}H NMR spectrum of compound **S3** in DMSO-d_6.

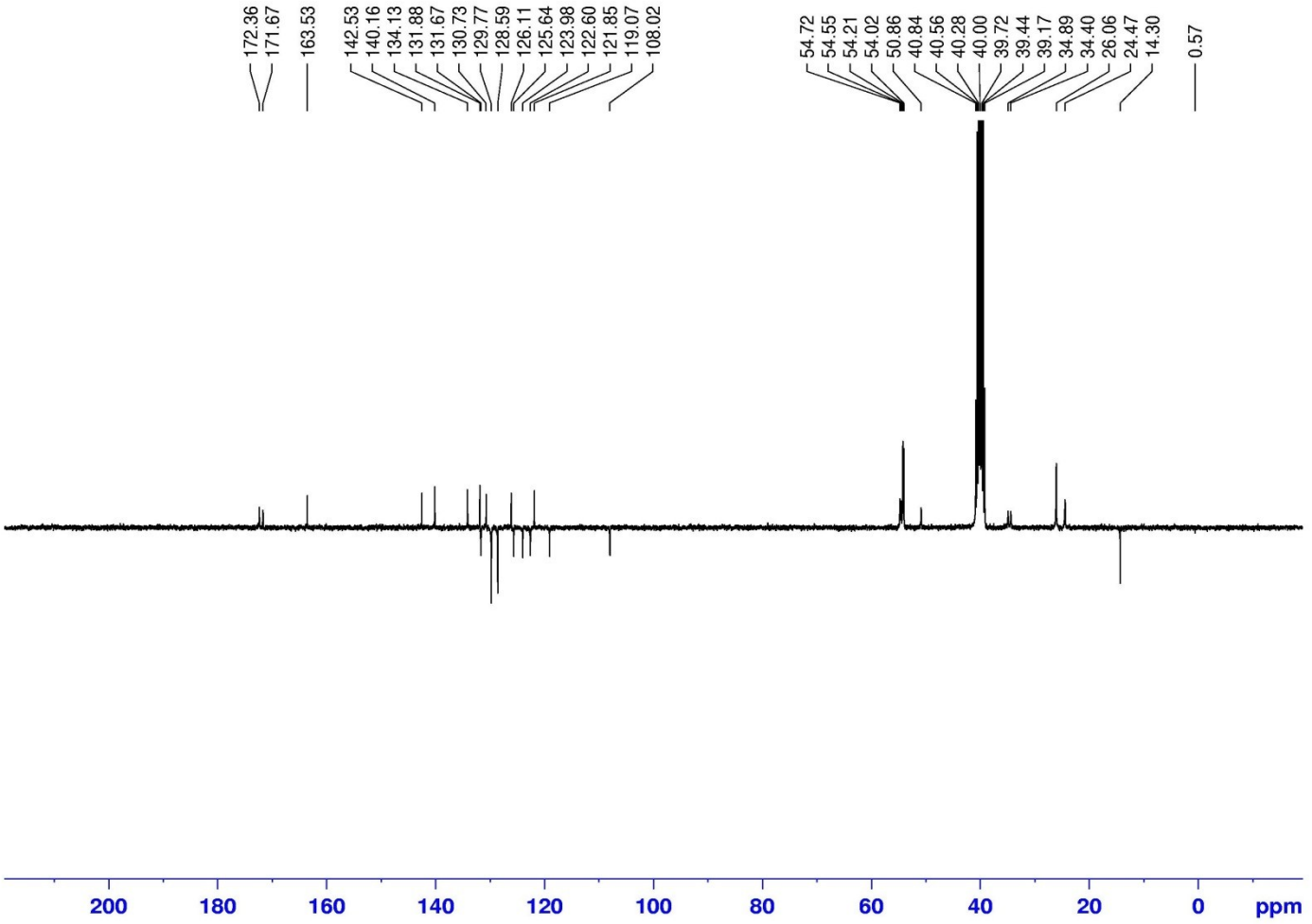

Figure S8: ^{13}C NMR spectrum of compound **S3** in DMSO-d_6.

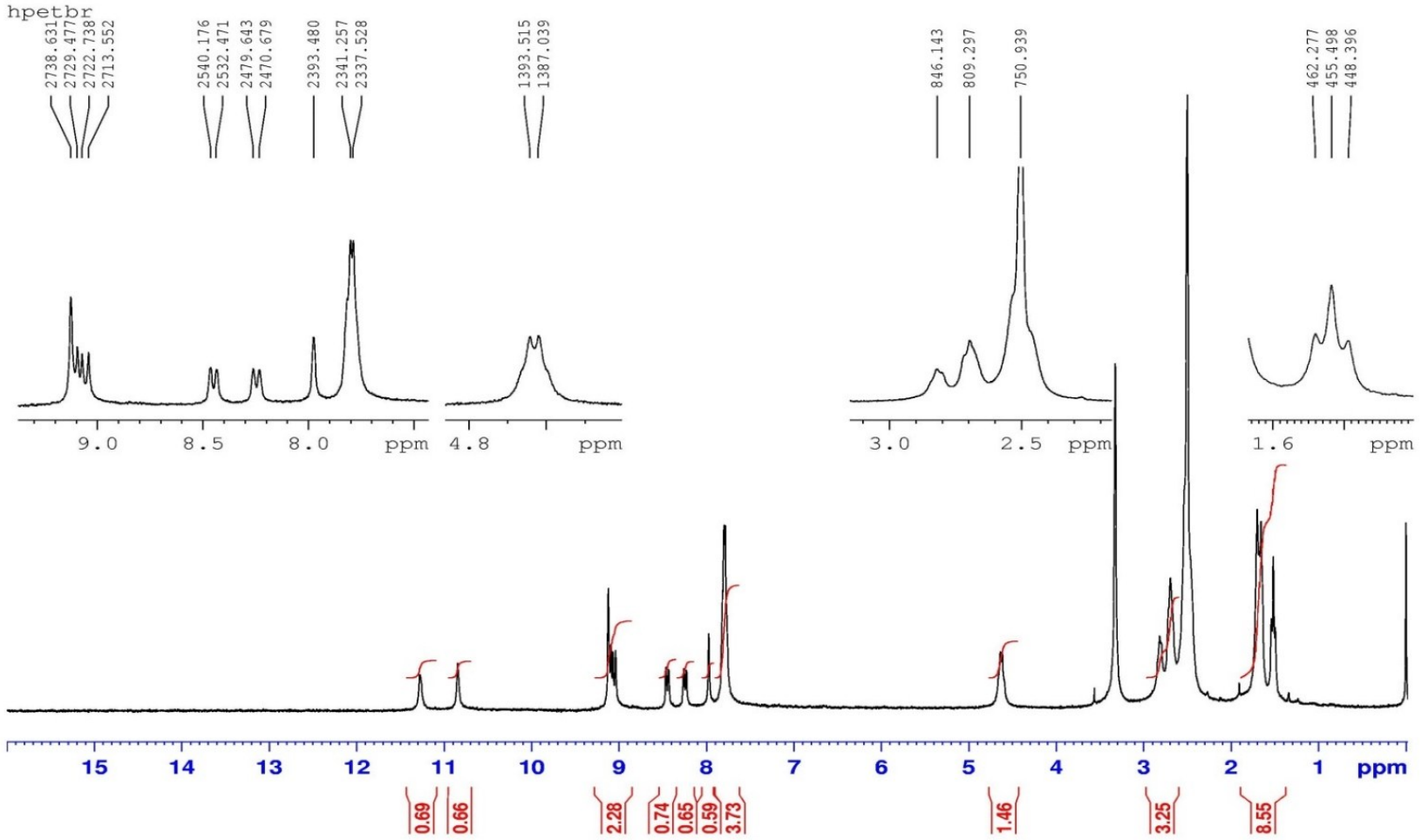

Figure S9. 1H NMR spectrum of compound S4 in DMSO-d6

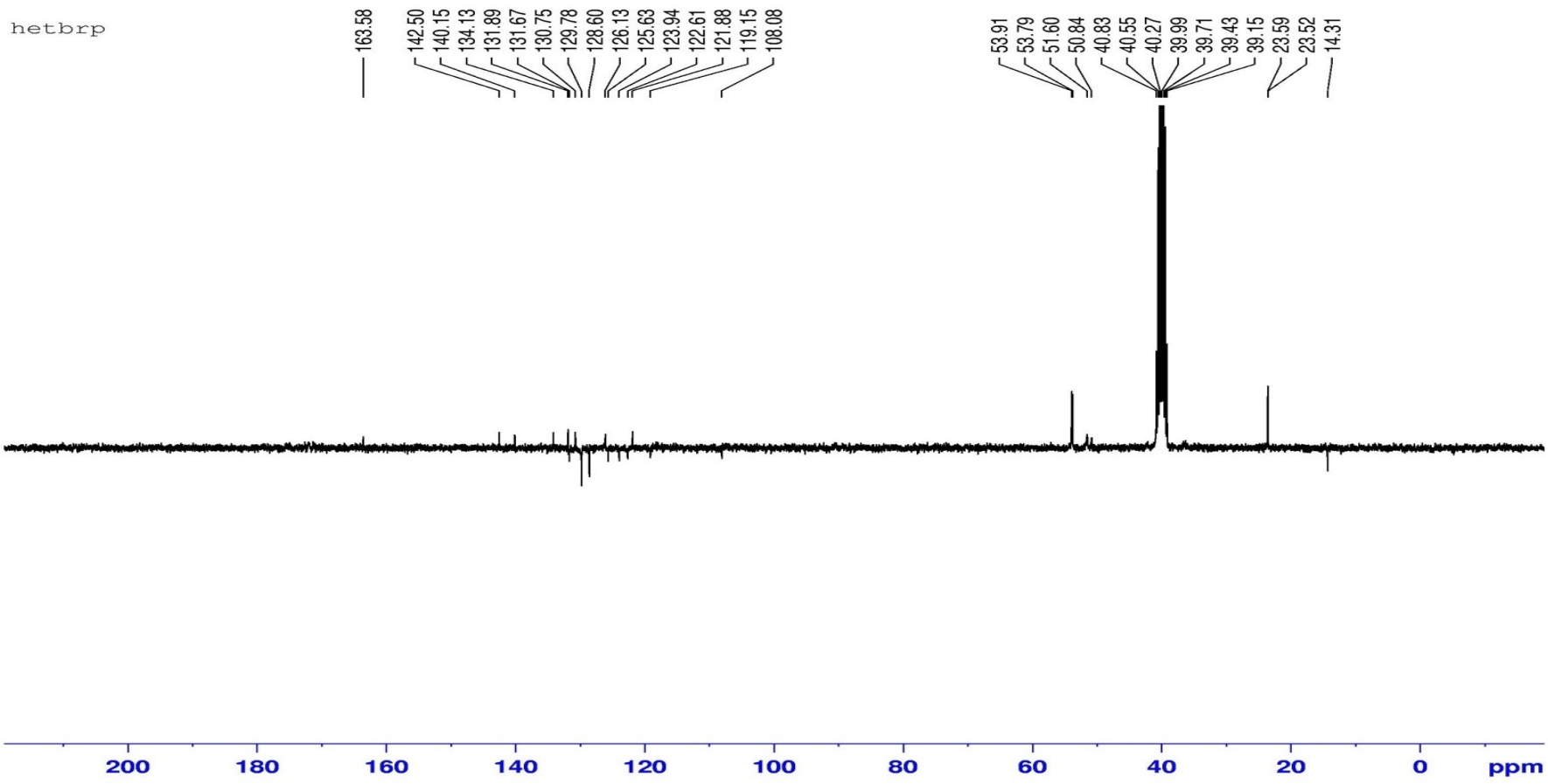

Figure S10: ^{13}C NMR spectrum of compound **S4** in DMSO-d_6.

HR-MS spectra

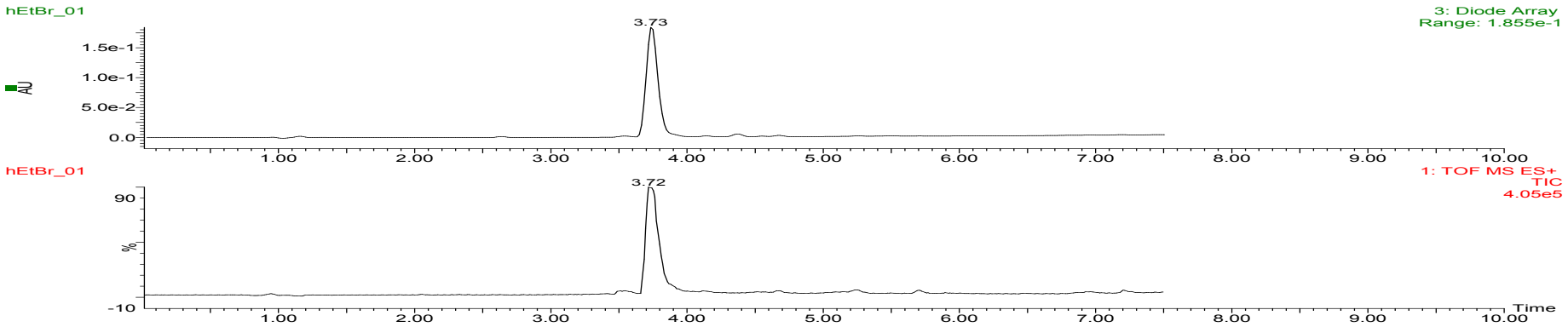

Single Mass Analysis
Tolerance = 5.0 PPM / DBE: min = -1.5, max = 50.0
Element prediction: Off
Number of isotope peaks used for i-FIT = 3
Monoisotopic Mass, Even Electron Ions
219 formula(e) evaluated with 1 results within limits (up to 50 closest results for each mass)
Elements Used:

Mass	Calc. Mass	mDa	PPM	DBE	Formula	i-FIT	i-FIT (Norm)	C	H	N	O	Cl
494.1401	494.1402	-0.1	-0.2	15.5	C27 H26 N3 O2 Cl2	156.9	0.0	27	26	3	2	2

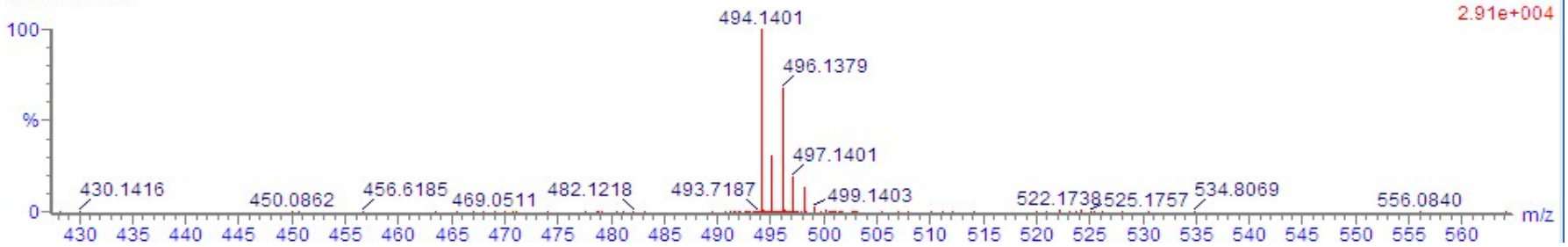

Figure S11: HR-MS spectrum of 3,8-bis(3-chloropropanamido)-5-ethyl-6-phenylphenanthridin-5-ium (**1**)

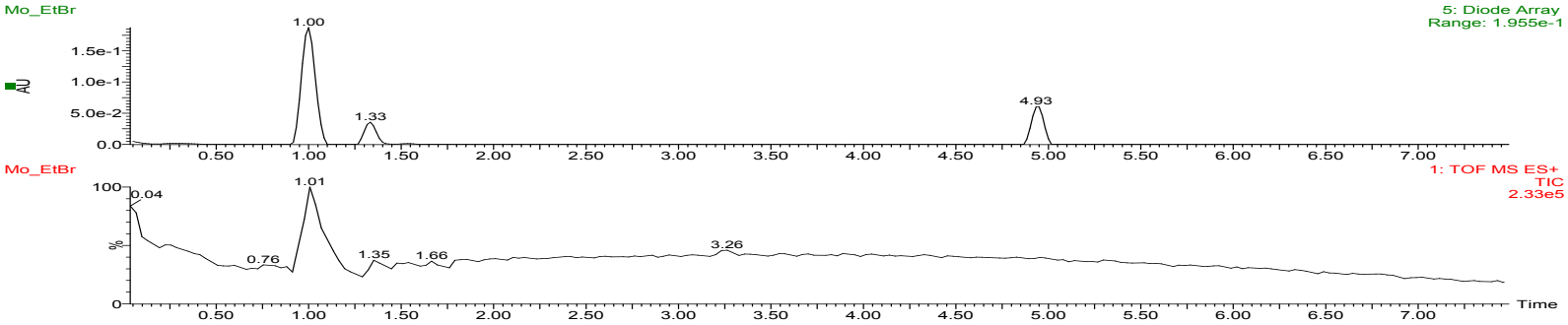

Single Mass Analysis

Tolerance = 5.0 PPM / DBE: min = -1.5, max = 50.0

Element prediction: Off

Number of isotope peaks used for i-FIT = 3

Monoisotopic Mass, Even Electron Ions

45 formula(e) evaluated with 1 results within limits (up to 50 closest results for each mass)

Elements Used:

Mass	Calc. Mass	mDa	PPM	DBE	Formula	i-FIT	i-FIT (Norm)	C	H	N	O
596.3246	596.3237	0.9	1.5	17.5	C35 H42 N5 O4	218.6	0.0	35	42	5	4

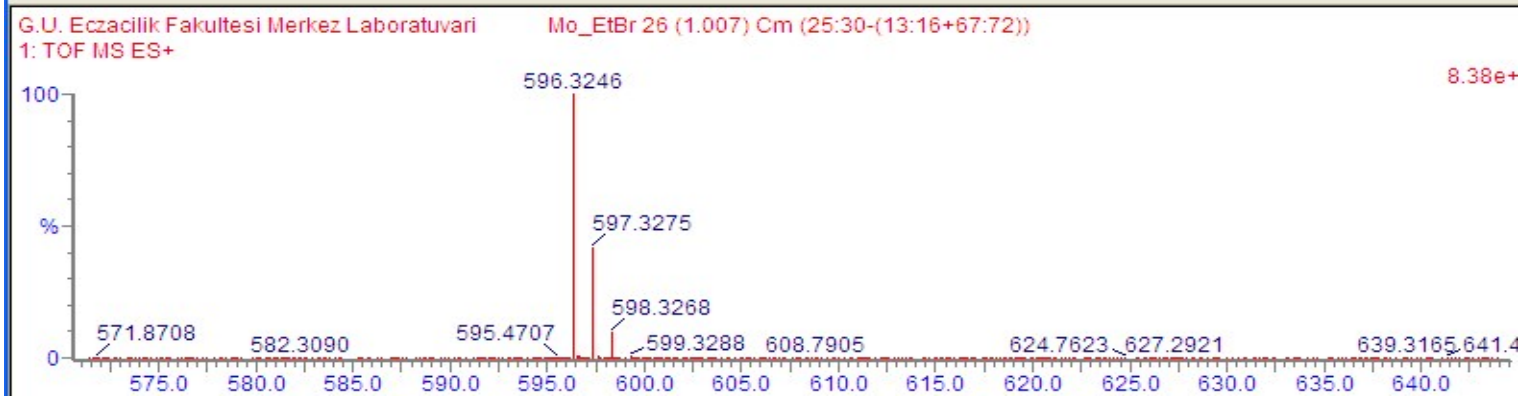

Figure S12: HR-MS spectrum of 5-ethyl-3,8-bis(3-morpholinopropanamido)-6-phenylphenanthridin-5-ium (**S1**)

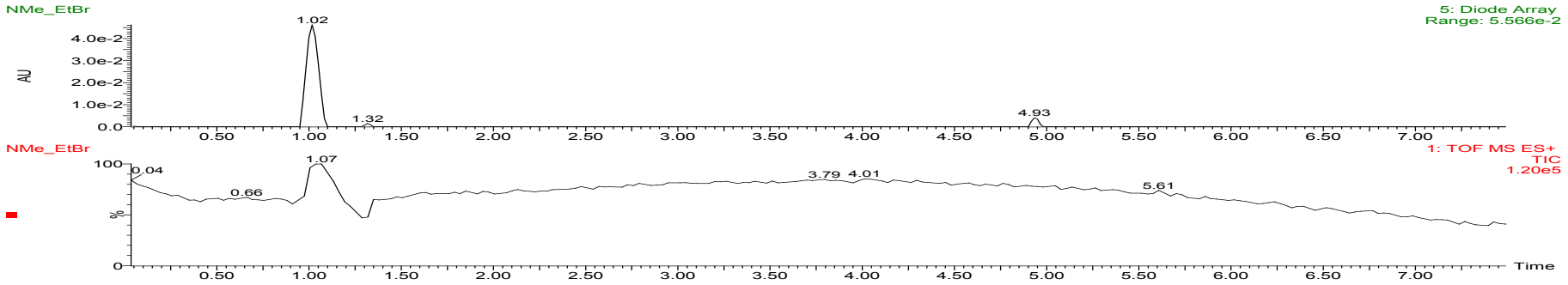

Single Mass Analysis

Tolerance = 5.0 PPM / DBE: min = -1.5, max = 50.0

Element prediction: Off

Number of isotope peaks used for i-FIT = 3

Monoisotopic Mass, Even Electron Ions

18 formula(e) evaluated with 1 results within limits (up to 50 closest results for each mass)

Elements Used:

Mass	Calc. Mass	mDa	PPM	DBE	Formula	i-FIT	i-FIT (Norm)	C	H	N	O
622.3875	622.3869	0.6	1.0	17.5	C37 H48 N7 O2	17.8	0.0	37	48	7	2

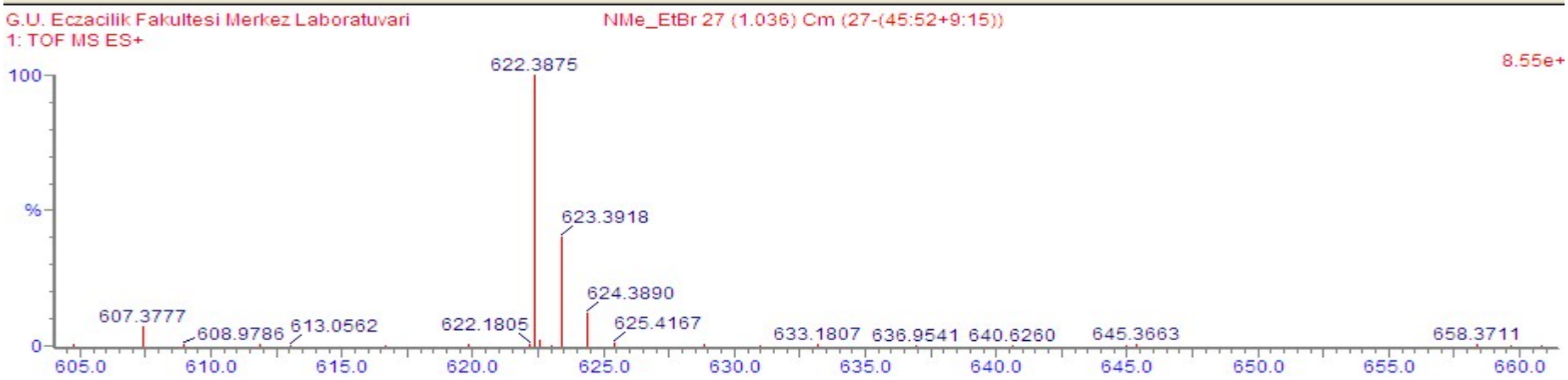

Figure S13: HR-MS spectrum of 5-ethyl-3,8-bis(3-(4-methylpiperazin-1-yl)propanamido)-6-phe nylphenanthridin-5-ium (**S2**)

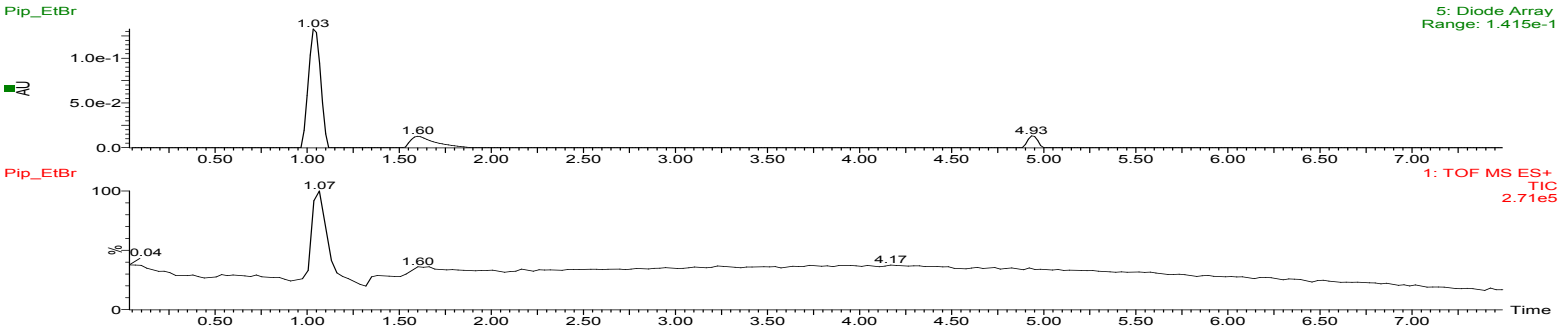

Single Mass Analysis

Tolerance = 5.0 PPM / DBE: min = -1.5, max = 50.0

Element prediction: Off

Number of isotope peaks used for i-FIT = 3

Monoisotopic Mass, Even Electron Ions

20 formula(e) evaluated with 1 results within limits (up to 50 closest results for each mass)

Elements Used:

Mass	Calc. Mass	mDa	PPM	DBE	Formula	i-FIT	i-FIT (Norm)	C	H	N	O
592.3663	592.3652	1.1	1.9	17.5	C37 H46 N5 O2	55.8	0.0	37	46	5	2

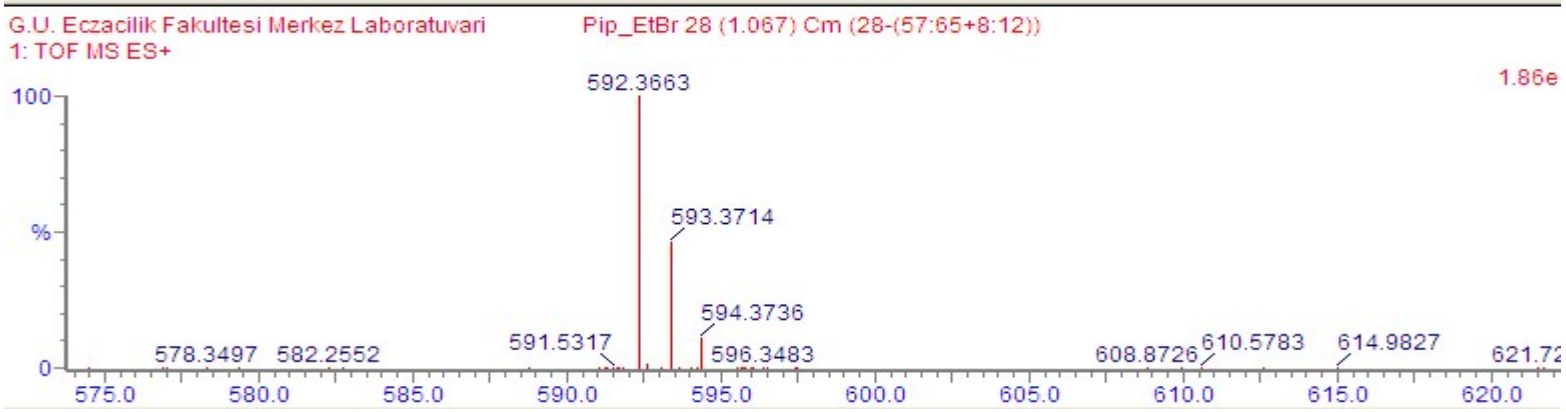

Figure S14: HR-MS spectrum of 5-ethyl-6-phenyl-3,8-bis(3-(piperidin-1-yl)propanamido)phenanthridin-5-ium (**S3**)

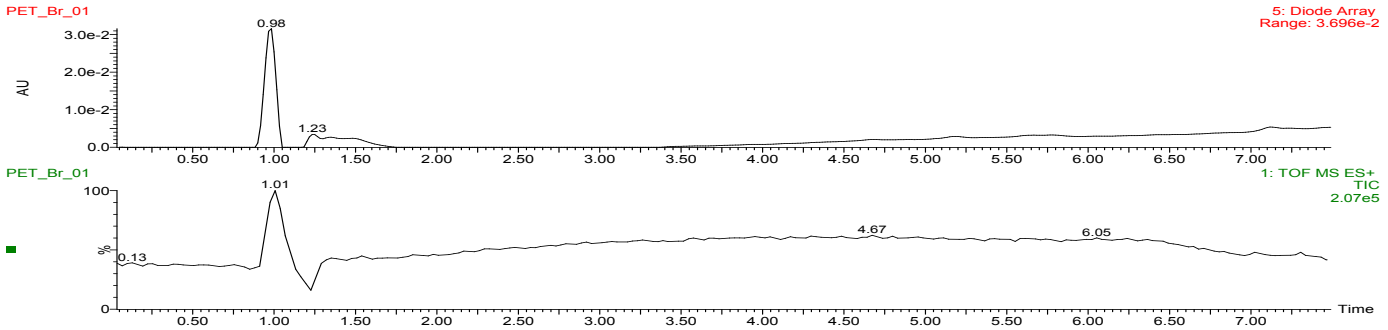

Single Mass Analysis

Tolerance = 5.0 PPM / DBE: min = -1.5, max = 50.0

Element prediction: Off

Number of isotope peaks used for i-FIT = 3

Monoisotopic Mass, Even Electron Ions

77 formula(e) evaluated with 1 results within limits (up to 50 closest results for each mass)

Elements Used:

Mass	Calc. Mass	mDa	PPM	DBE	Formula	i-FIT	i-FIT (Norm)	C	H	N	O
564.3344	564.3339	0.5	0.9	17.5	C35 H42 N5 O2	95.8	0.0	35	42	5	2

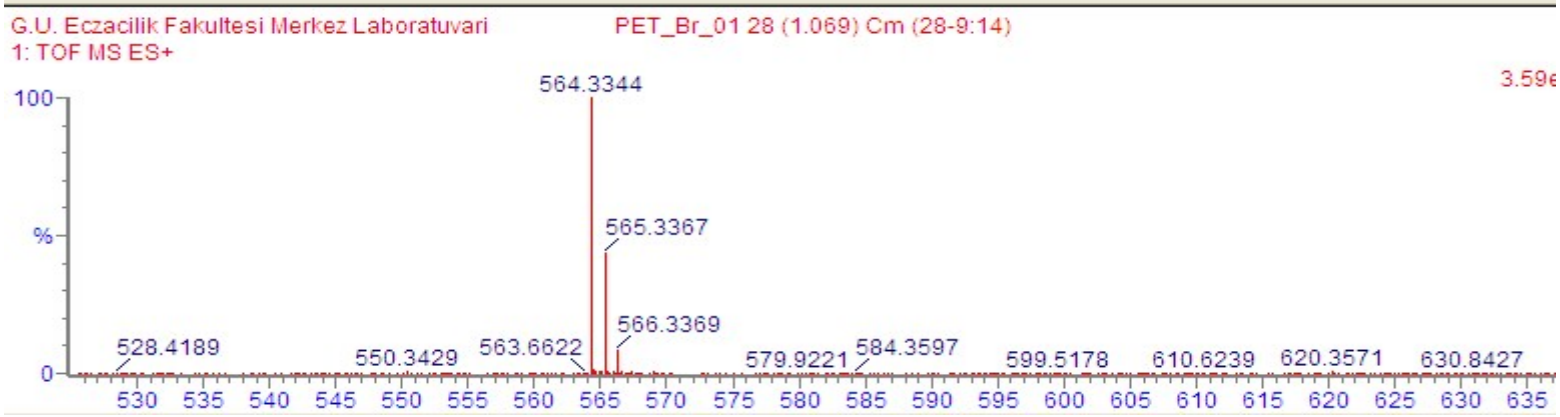

Figure S15: HR-MS spectrum of 5-ethyl-6-phenyl-3,8-bis(3-(pyrrolidin-1-yl)propanamido)phenanthridin-5-ium (**S4**)

Fluorescence and UV-Vis absorption titrations

For fluorescence titrations stock solutions of chemosensors were prepared in acetonitrile. Meldonium (10 mM) was dissolved in methanol and ignorable volume of analyte was added during titrations. Other analytes were dissolved in acetonitrile. Measurements were taken in a quartz fluorescence cuvette with 1cm-path length. Excitation wavelengths were selected using lowest energy isosbestic points of UV-Vis titrations. S1-S4 were prepared as 20 µM in acetonitrile while meldonium (10 mM) was prepared in methanol in UV-Vis titrations.

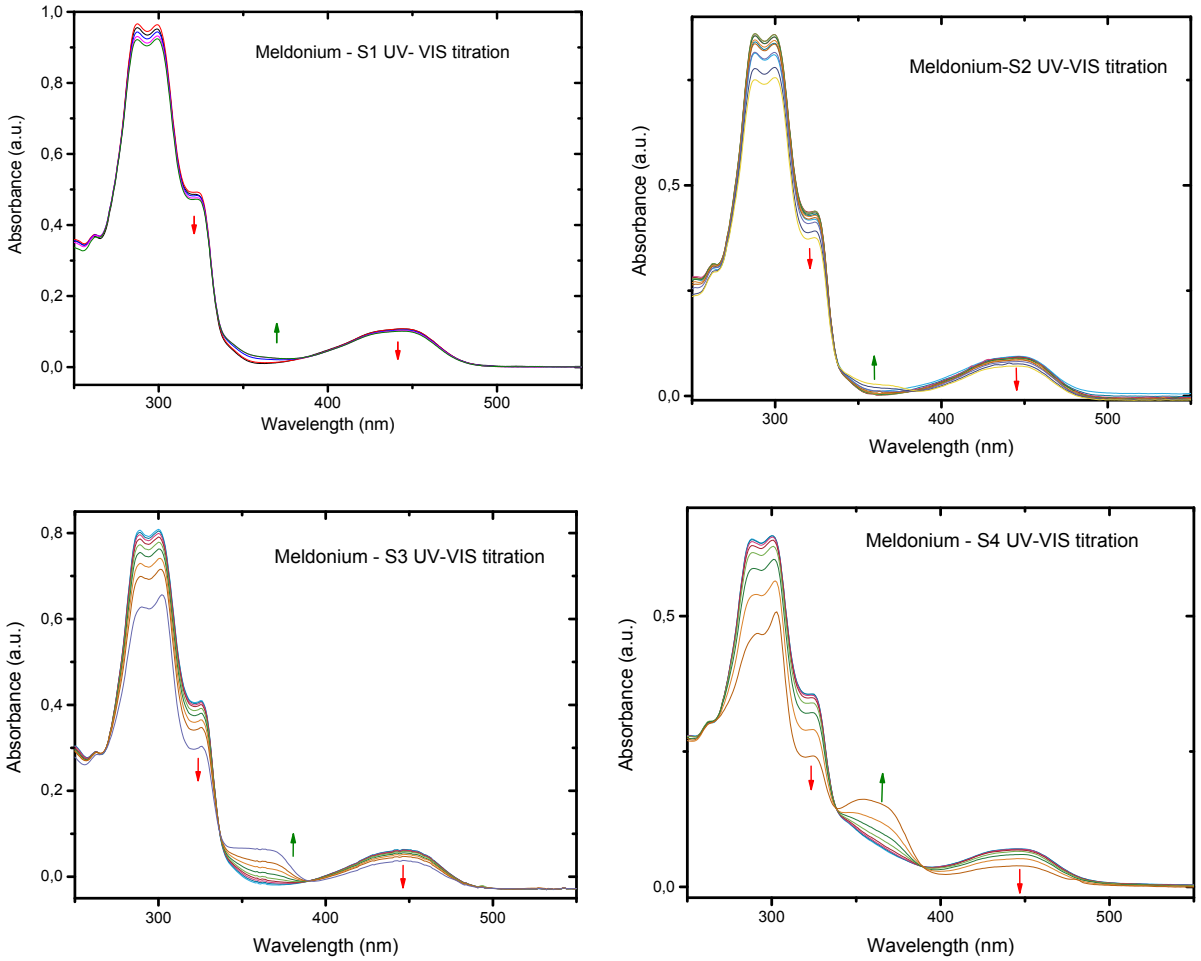

Figure S16. UV-VIS titration spectra of meldonium

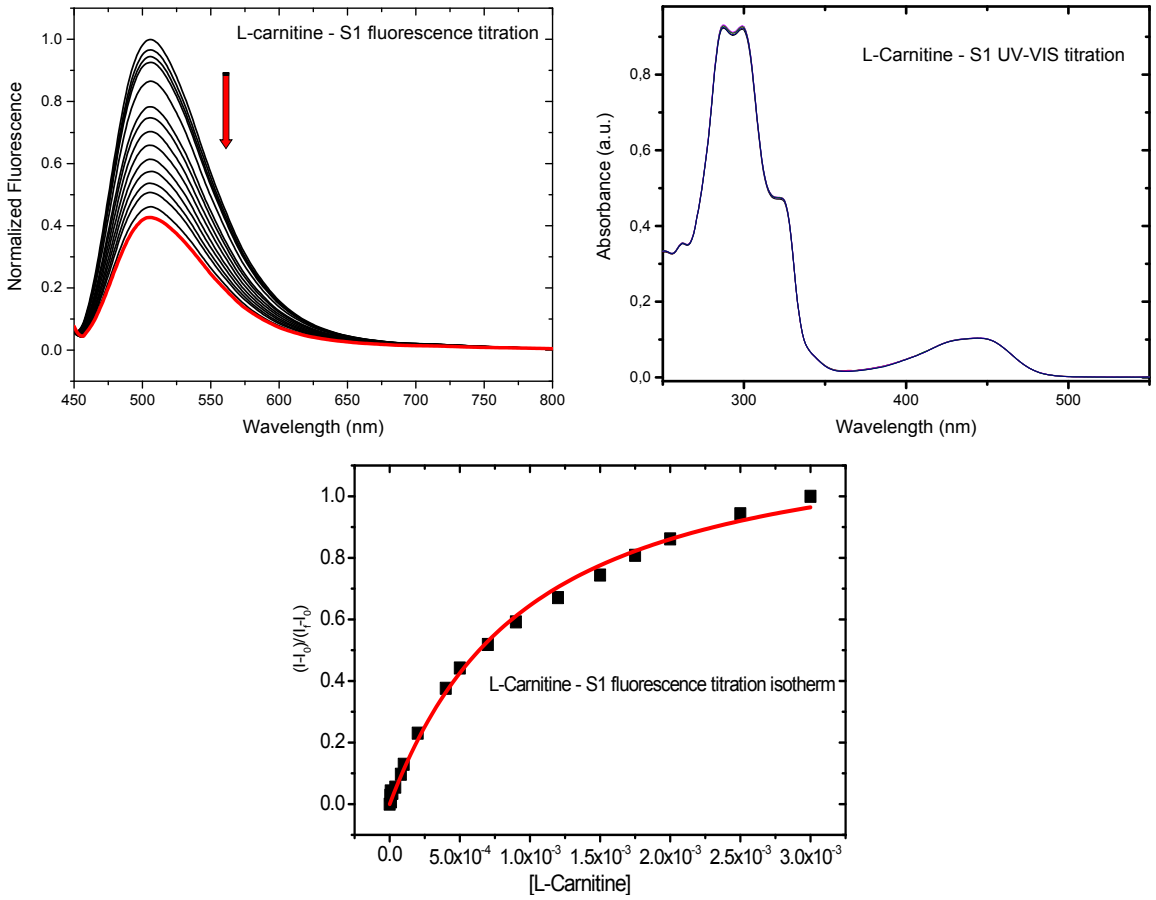

Figure S17. Fluorescence spectra (above left) and binding isotherms (bottom) of L-carnitine-**S1** fluorescence titrations (λ_{exc}=438 nm) and UV-Vis spectra of carnitine-**S1** titration (above right).

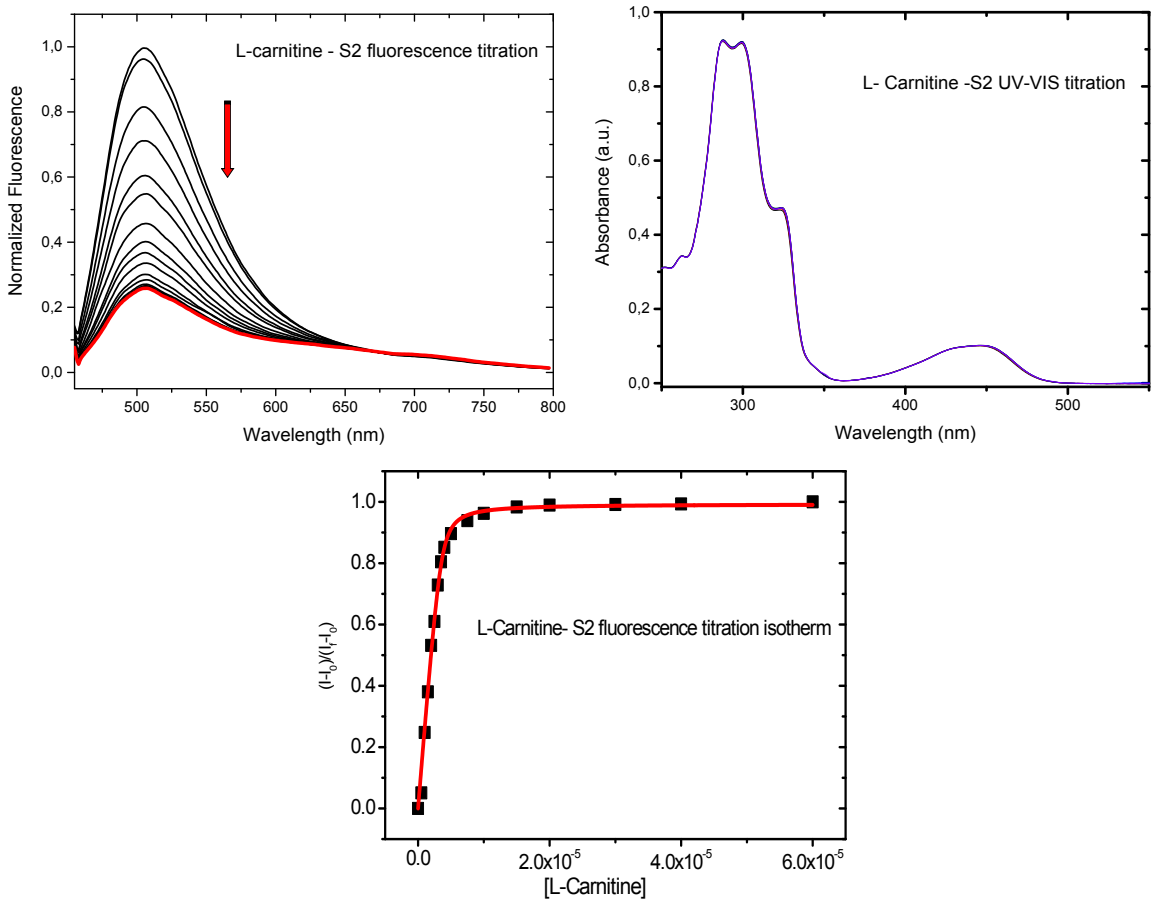

Figure S18. Fluorescence spectra (above left) and binding isotherms (bottom) of L-carnitine – **S2** fluorescence titrations (λ_{exc}=443 nm) and UV-Vis spectra of L-carnitine-**S2** titration (above right).

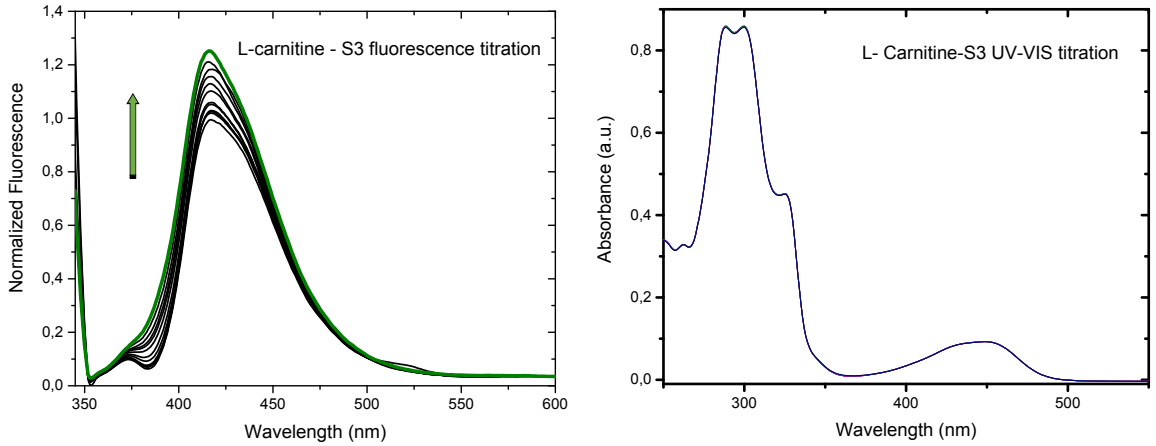

Figure S19. Fluorescence spectra (left) of L-carnitine – **S3** fluorescence titrations (λ_{exc}=336 nm) and UV-Vis spectra of L-carnitine-**S3** titration (right).

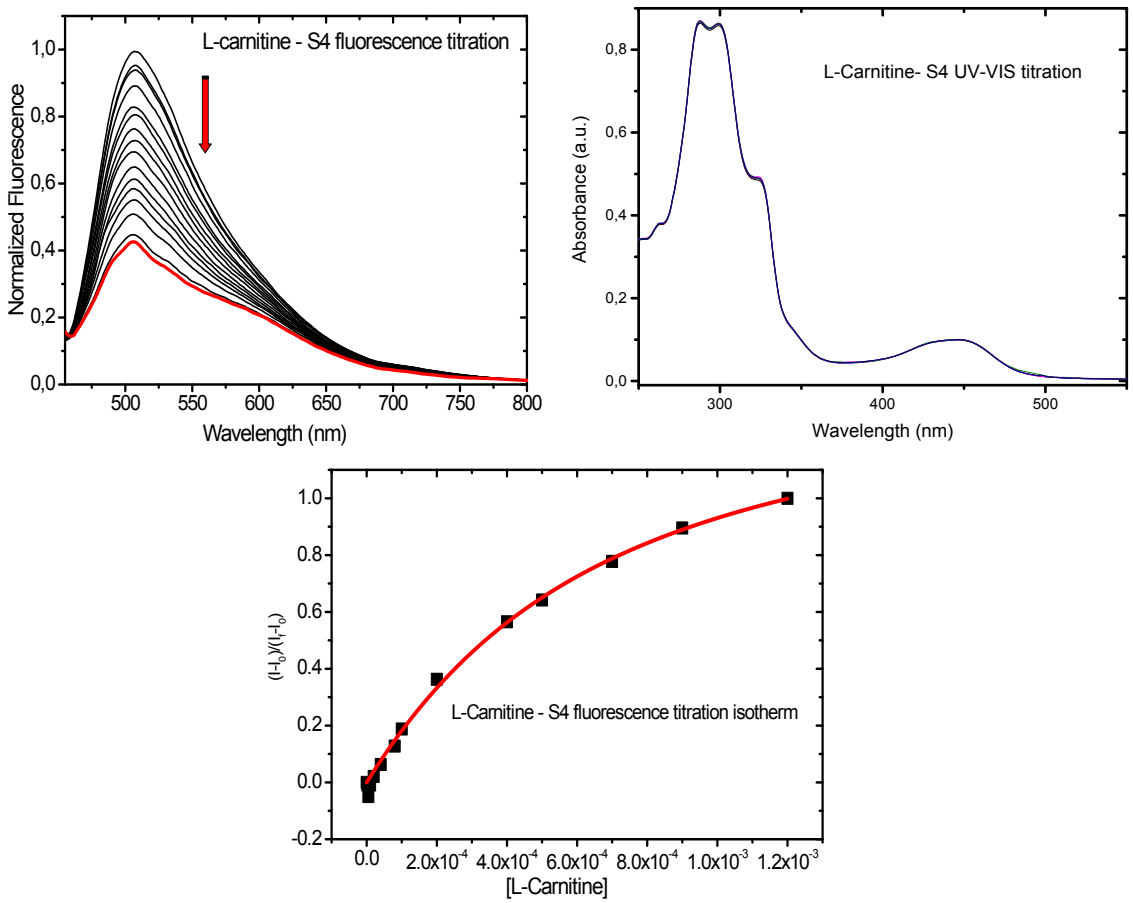

Figure S20. Fluorescence spectra (above left) and binding isotherms (bottom) of L-carnitine – **S4** fluorescence titrations (λ_{exc}=440 nm) and UV-Vis spectra of L-carnitine-**S4** titration (above right).

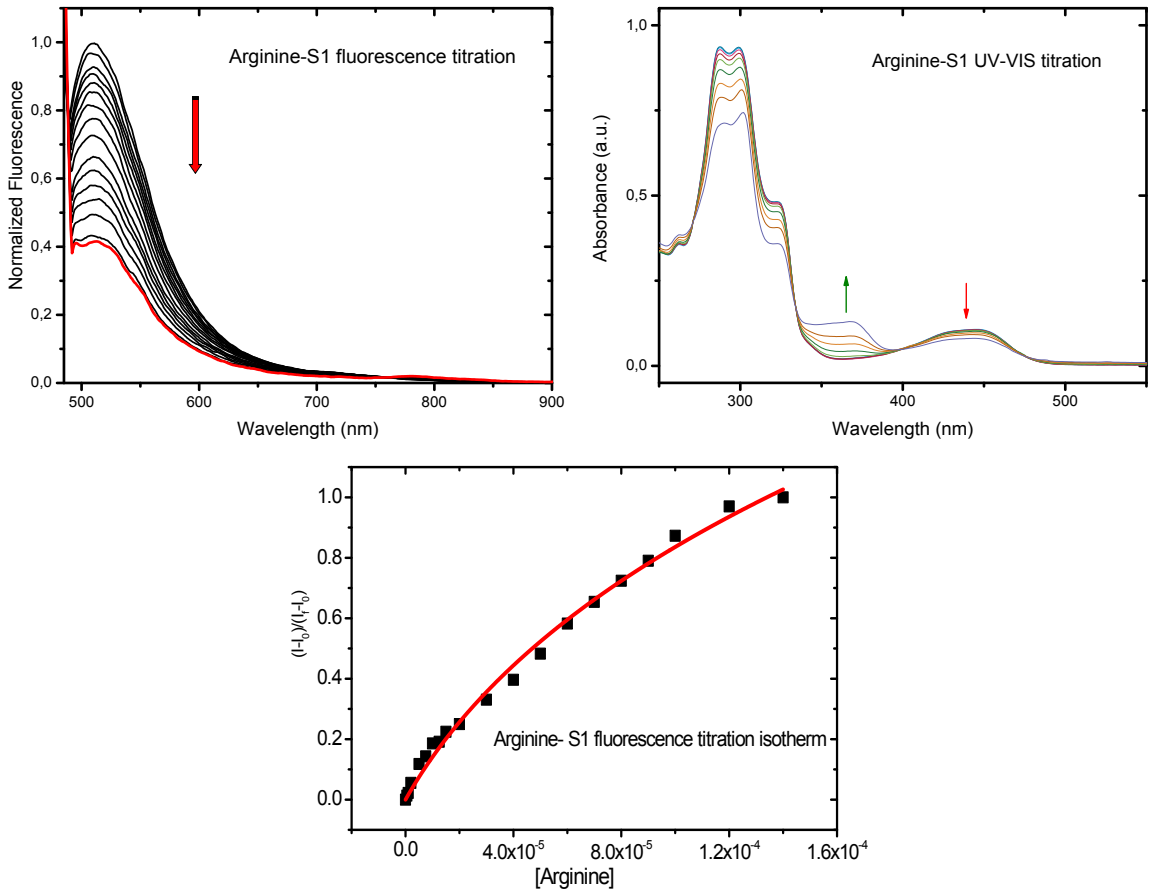

Figure S21. Fluorescence spectra (above left) and binding isotherms (bottom) of arginine– **S1** (20 μM) fluorescence titrations (λ_{exc}=473 nm) and UV-Vis spectra of arginine –**S1** titration (above right).

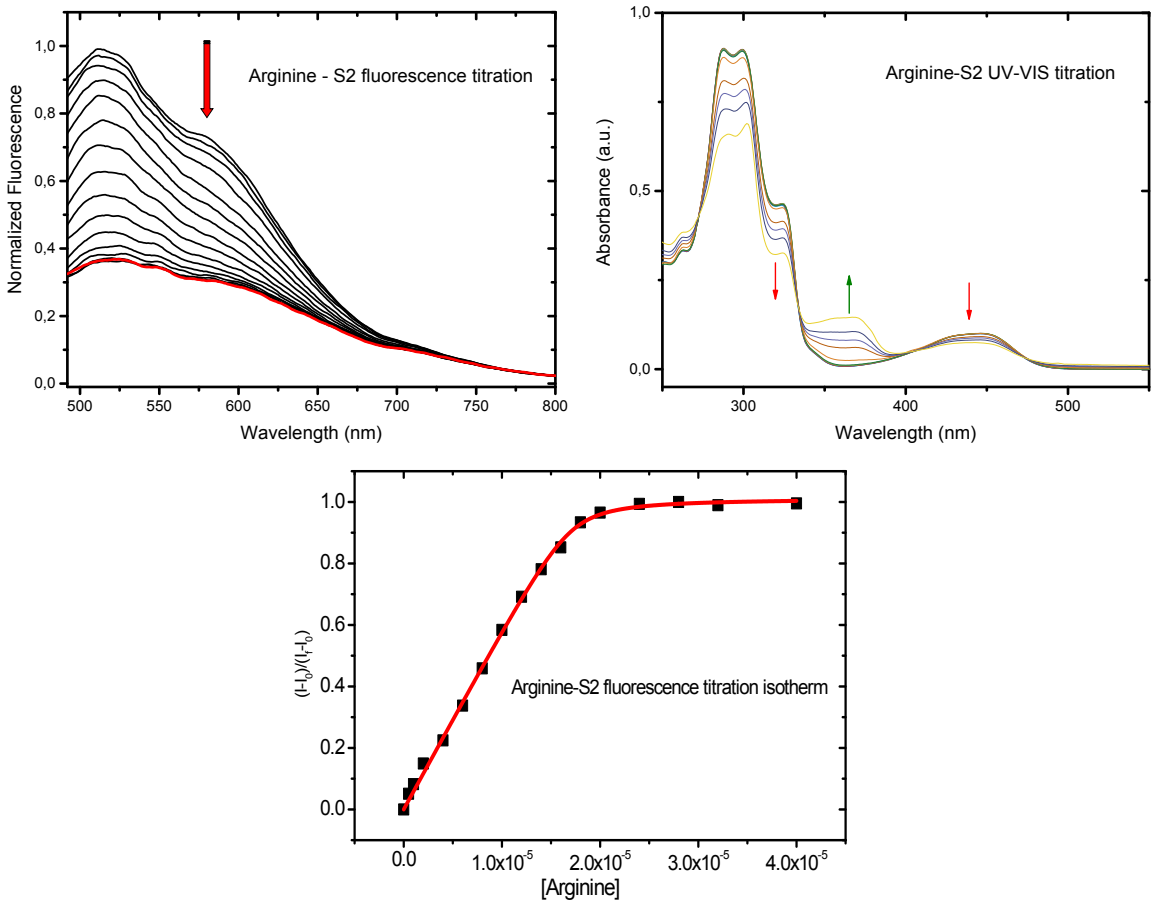

Figure S22. Fluorescence spectra (above left) and binding isotherms (bottom) of arginine– **S2** (40 μM) fluorescence titrations (λ_{exc}=473 nm) and UV-Vis spectra of arginine –**S2** titration (above right).

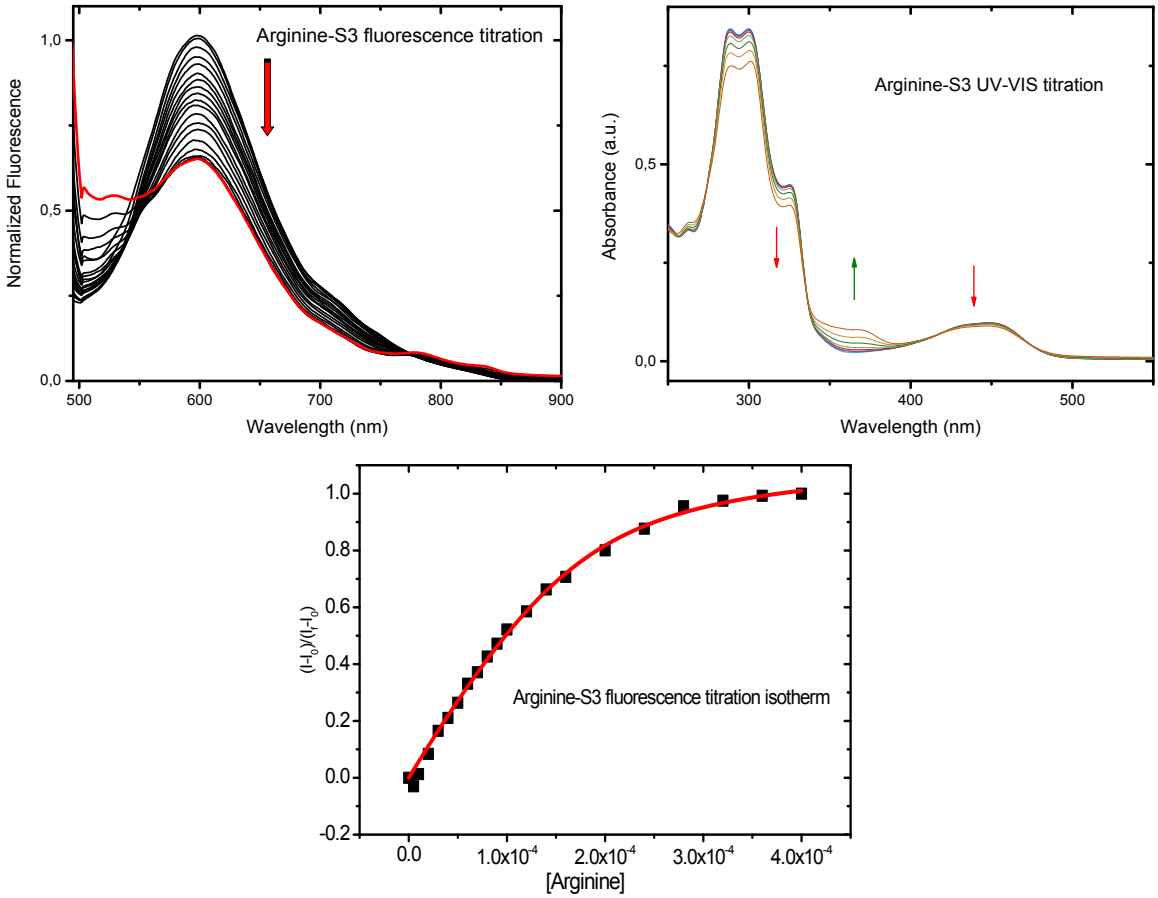

Figure S23. Fluorescence spectra (above left) and binding isotherms (bottom) of arginine– **S3** (60 μM) fluorescence titrations (λ_{exc}=474 nm) and UV-Vis spectra of arginine –**S3** titration (above right).

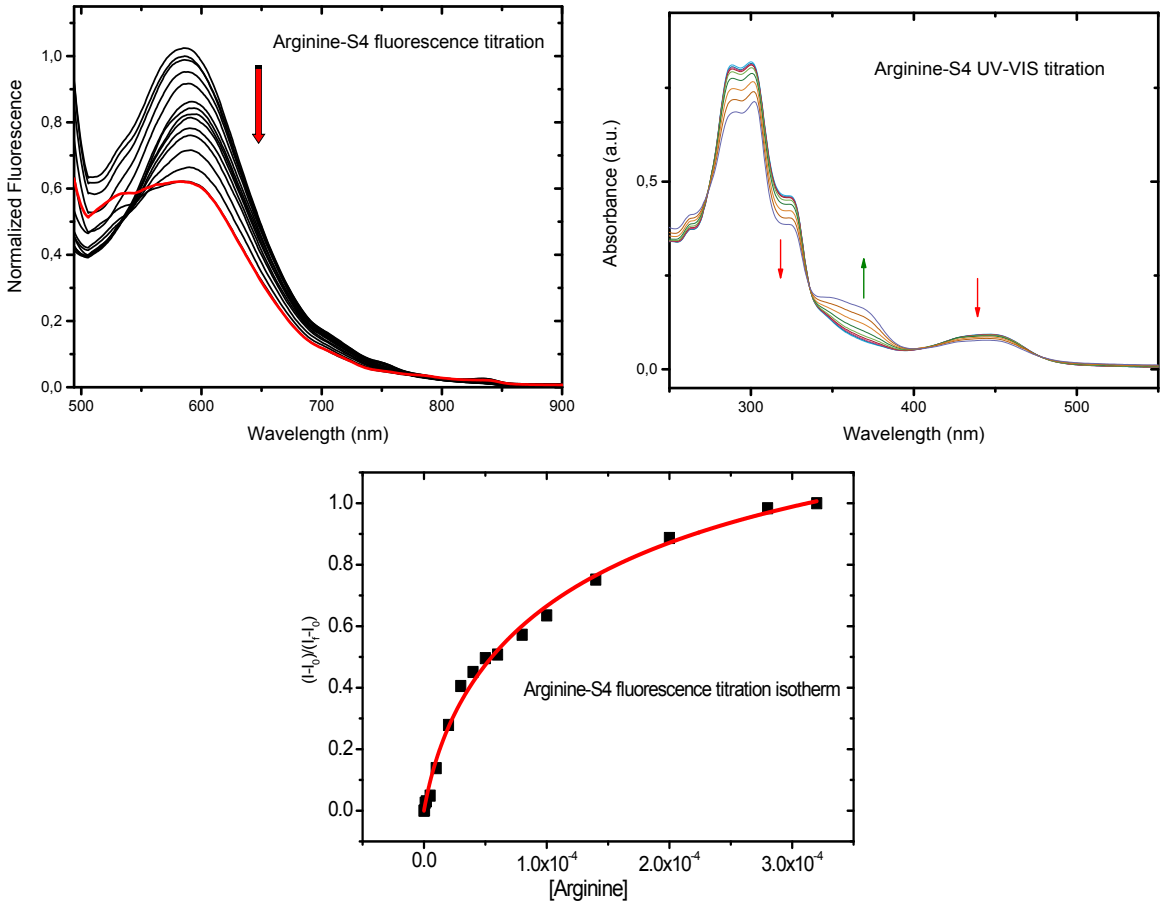

Figure S24. Fluorescence spectra (above left) and binding isotherms (bottom) of arginine– **S4** (50 μM) fluorescence titrations (λ_{exc}=477 nm) and UV-Vis spectra of arginine –**S4** titration (above right).

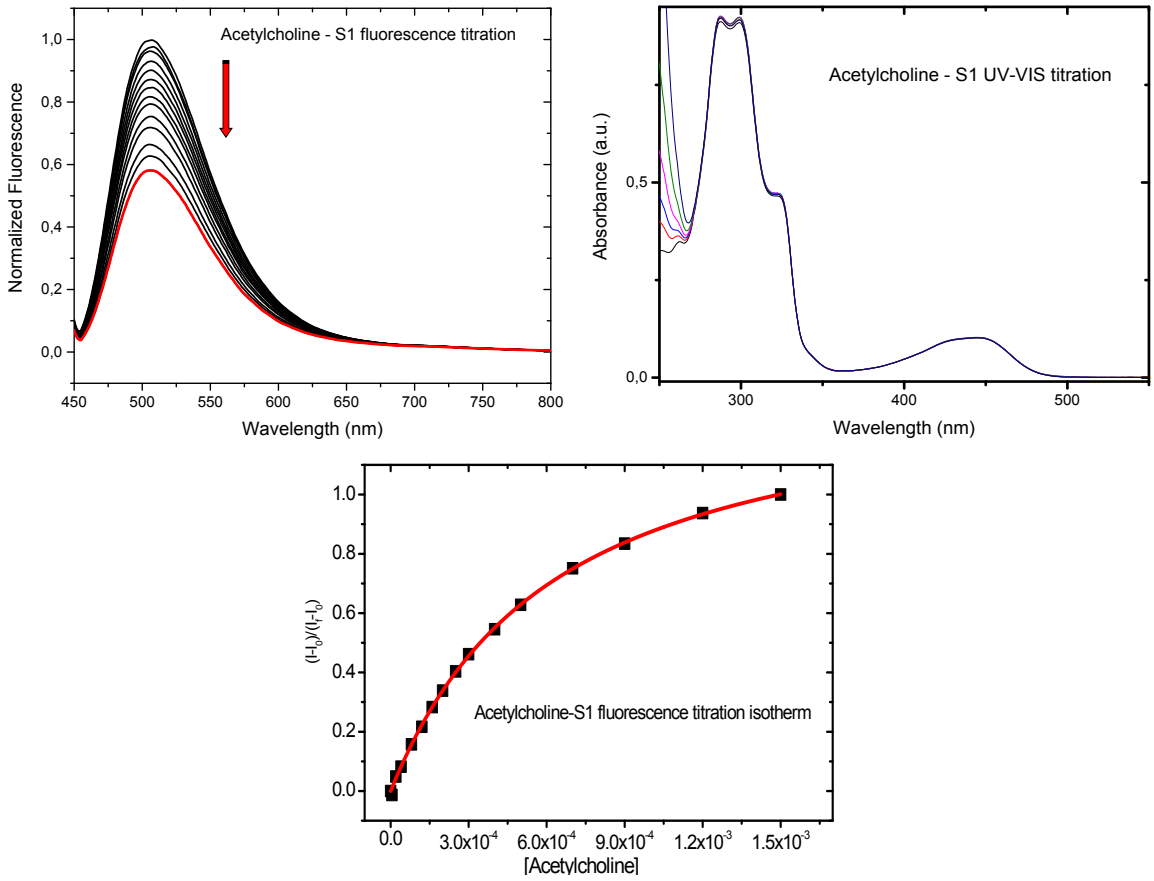

Figure S25. Fluorescence spectra (above left) and binding isotherms (bottom) of acetylcholine– **S1** (20 μM) fluorescence titrations (λ_{exc}=438 nm) and UV-Vis spectra of acetylcholine –**S1** titration (above right).

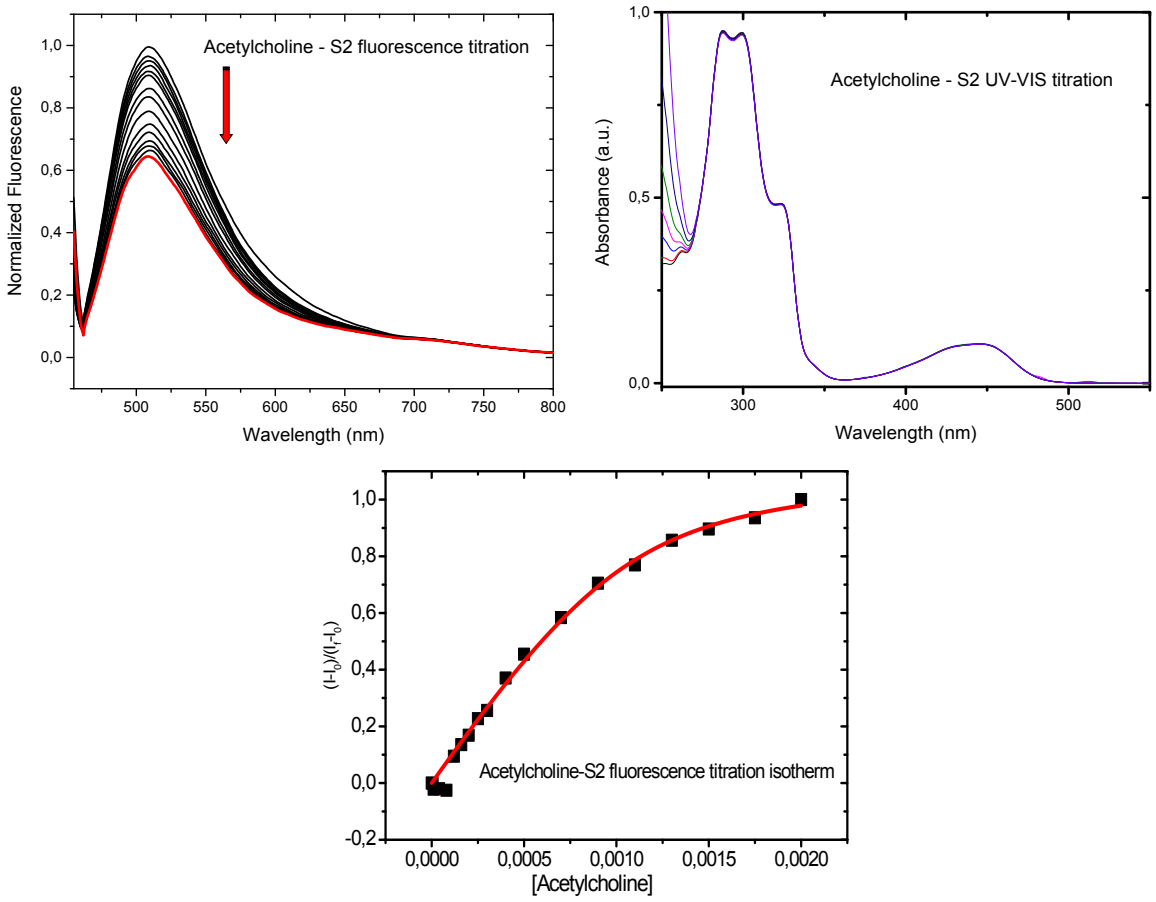

Figure S26. Fluorescence spectra (above left) and binding isotherms (bottom) of acetylcholine– **S2** (20 μM) fluorescence titrations (λ_{exc}=443 nm) and UV-Vis spectra of acetylcholine–**S2** titration (above right).

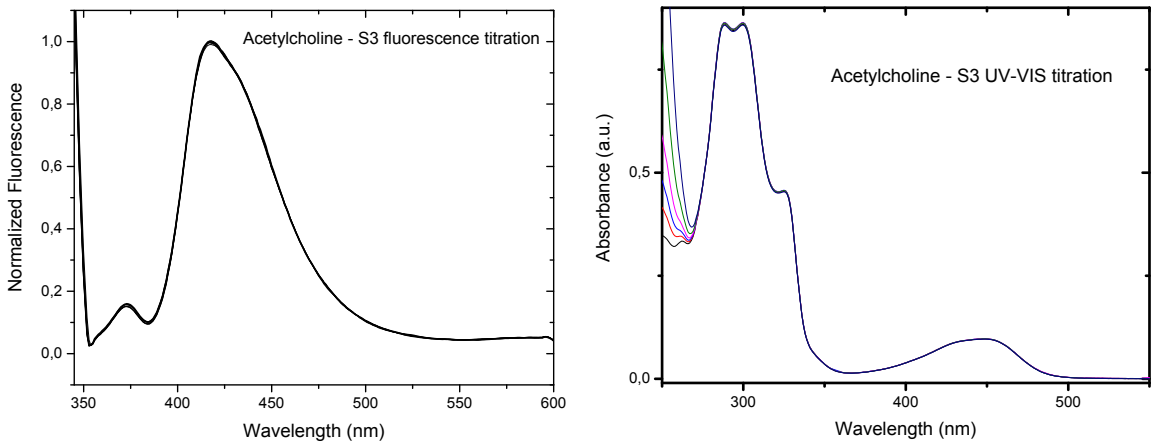

Figure S27. Fluorescence spectra (left) of acetylcholine– **S3** (2 μM) fluorescence titration (λ_{exc}=336 nm) and UV-Vis spectra of acetylcholine –**S3** titration (right).

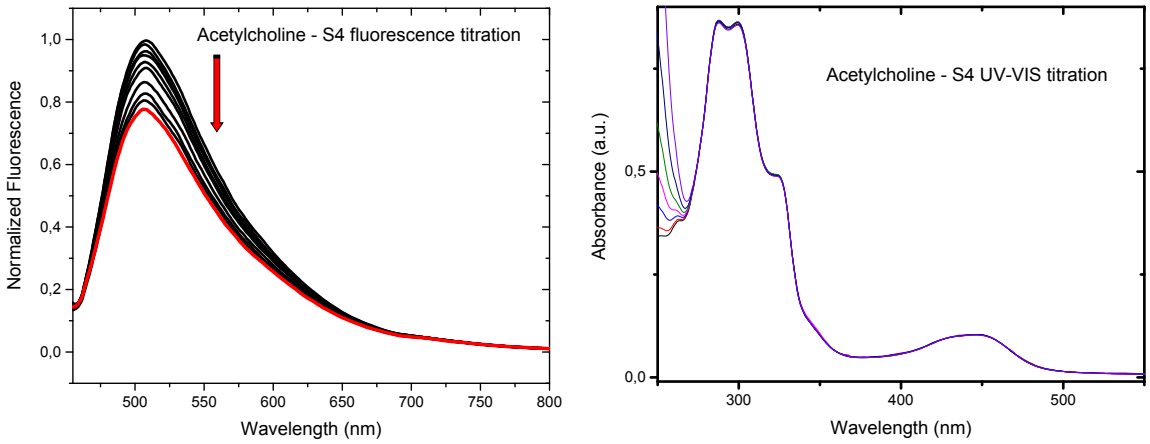

Figure S28. Fluorescence spectra (left) of acetylcholine– **S4** (25 µM) fluorescence titration (λ_{exc}=440 nm) and UV-Vis spectra of acetylcholine –**S4** titration (right).

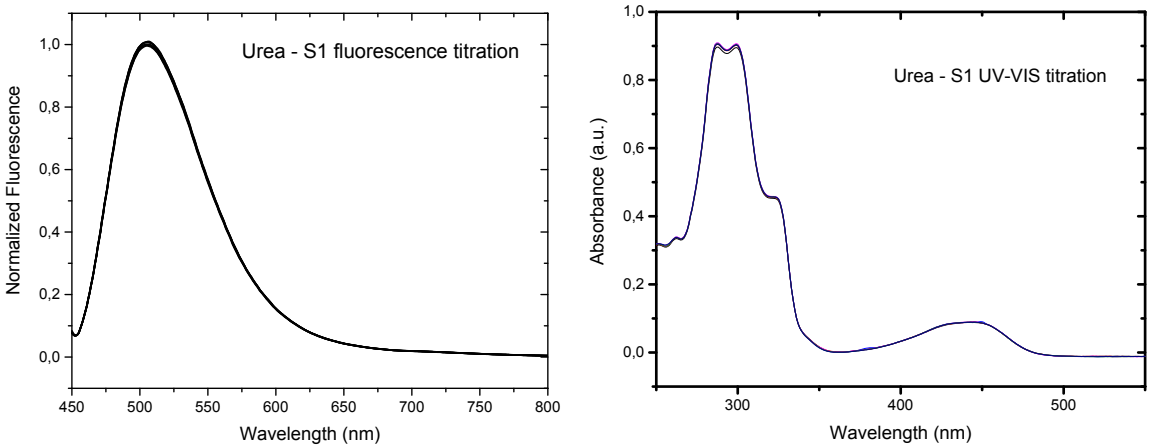

Figure S29. Fluorescence spectra (left) of urea– **S1** (20 µM) fluorescence titration (λ_{exc}=438 nm) and UV-Vis spectra of urea –**S1** titration (right).

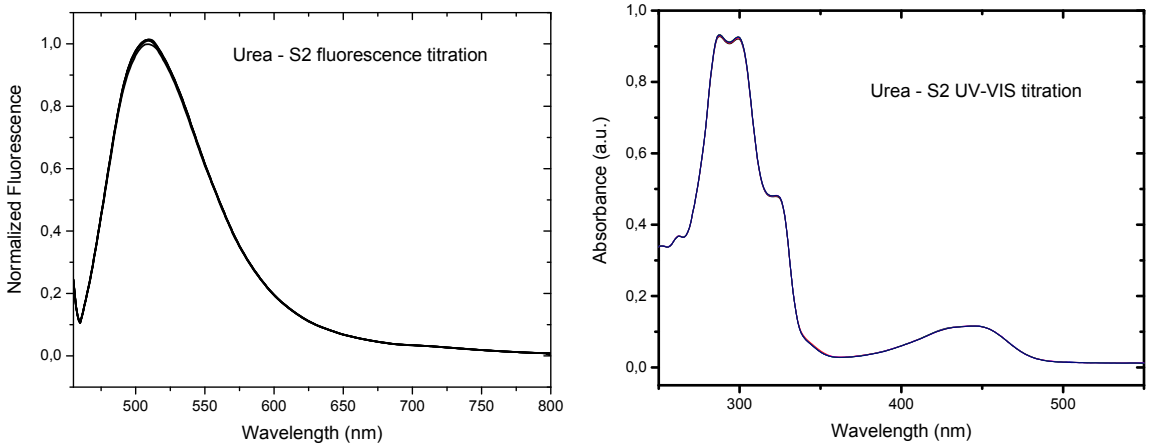

Figure S30. Fluorescence spectra (left) of urea– **S2** (20 µM) fluorescence titration (λ_{exc}=443 nm) and UV-Vis spectra of urea –**S2** titration (right).

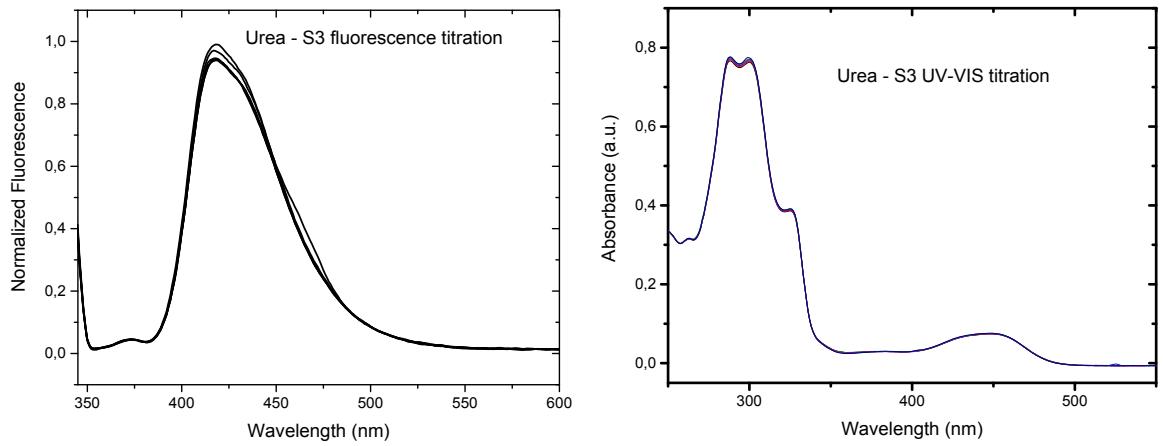

Figure S31. Fluorescence spectra (left) of urea– **S3** (2 μM) fluorescence titration (λ_{exc}=336 nm) and UV-Vis spectra of urea –**S3** titration (right).

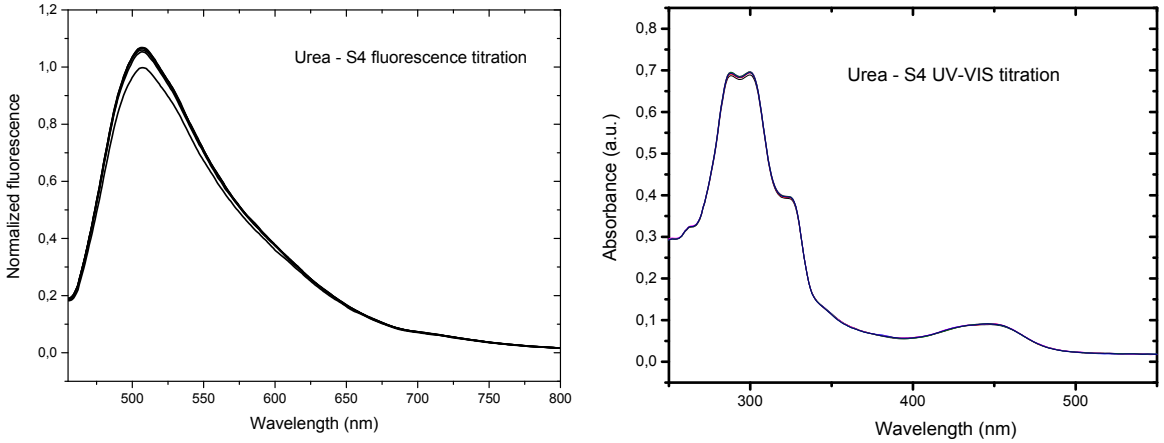

Figure S32. Fluorescence spectra (left) of urea– **S4** (25 μM) fluorescence titration (λ_{exc}=440 nm) and UV-Vis spectra of urea –**S4** titration (right).

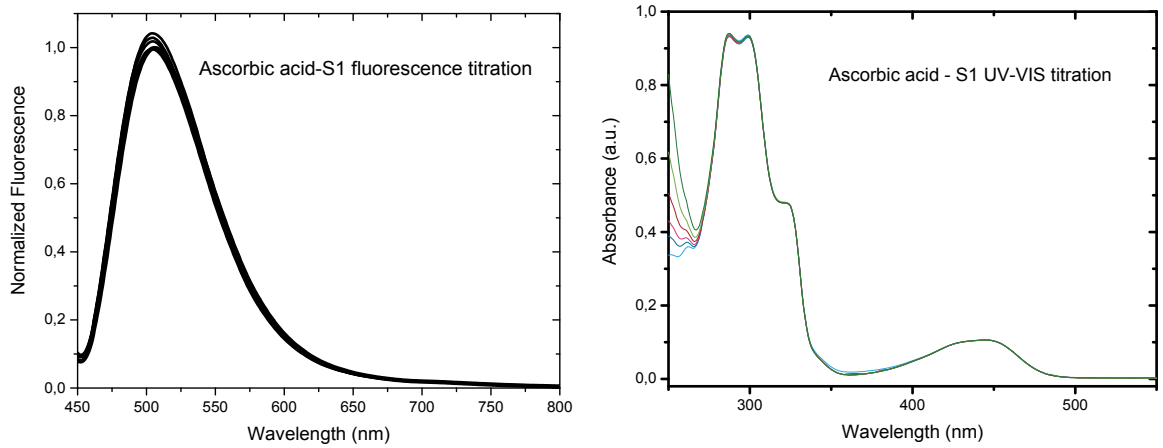

Figure S33. Fluorescence spectra (left) of ascorbic acid– **S1** (20 μM) fluorescence titration (λ_{exc}=438 nm) and UV-Vis spectra of ascorbic acid–**S1** titration (right).

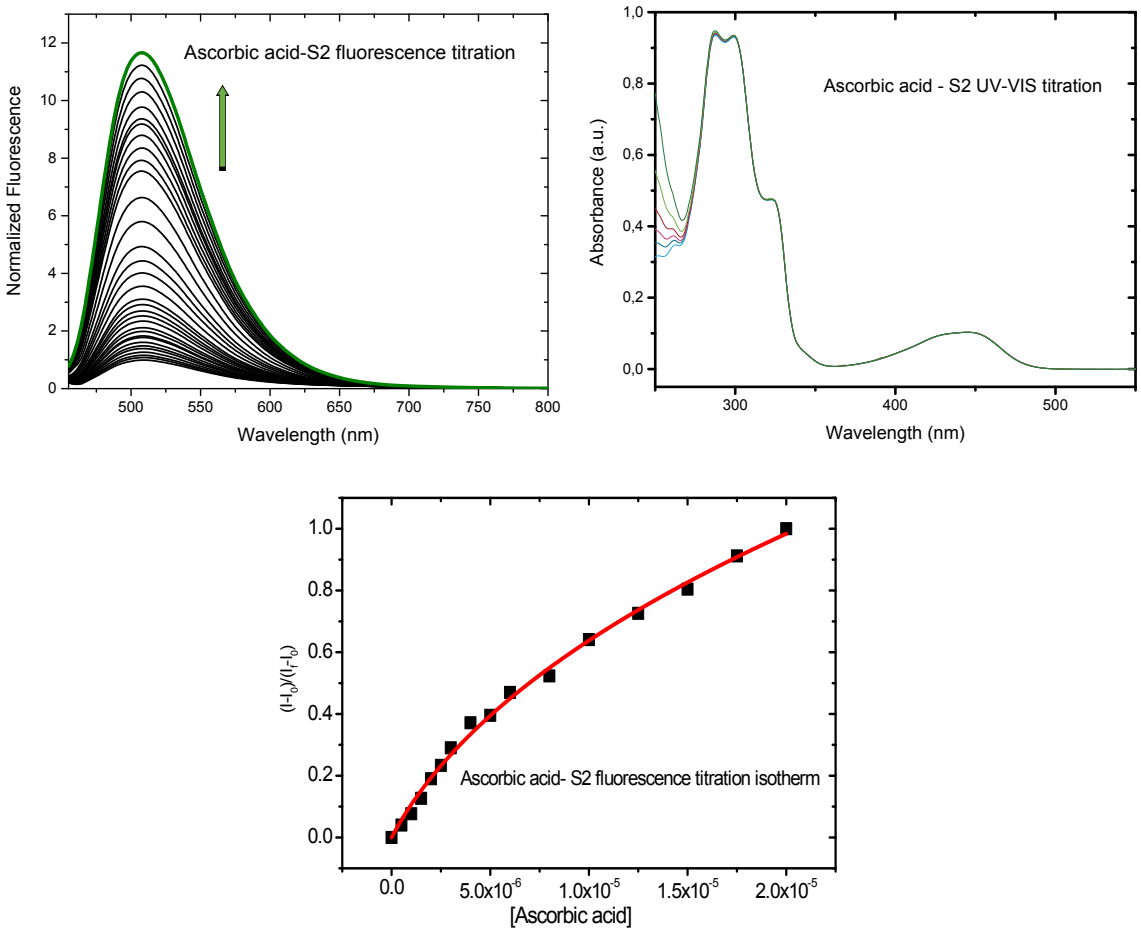

Figure S34. Fluorescence spectra (above left) and binding isotherms (bottom) of ascorbic acid– **S2** (20 μM) fluorescence titration (λ_{exc}=443 nm) and UV-Vis spectra of ascorbic acid –S2 titration (above right).

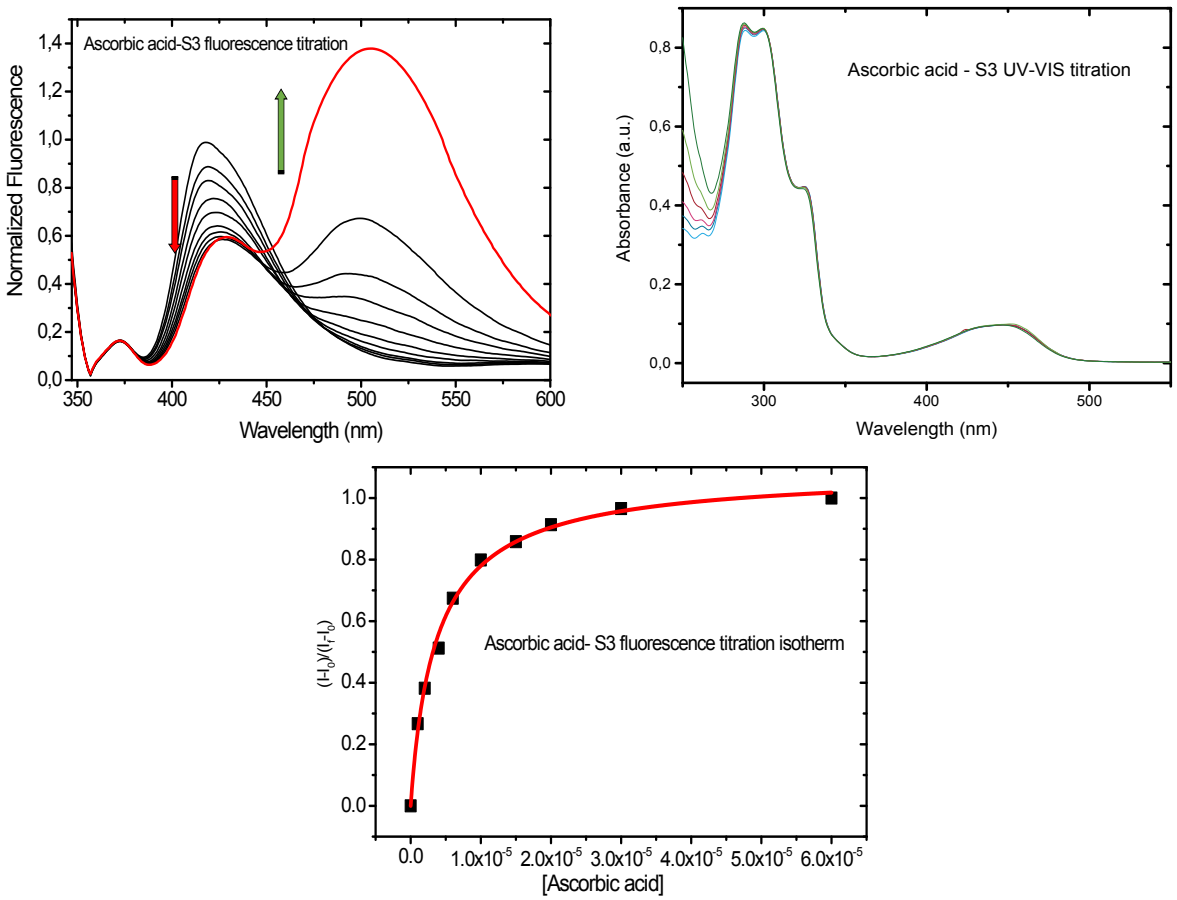

Figure S35. 4. Fluorescence spectra (above left) and binding isotherms (bottom) of ascorbic acid– **S3** (2 µM) fluorescence titration (λexc=336 nm) and UV-Vis spectra of ascorbic acid –**S3** titration (above right).

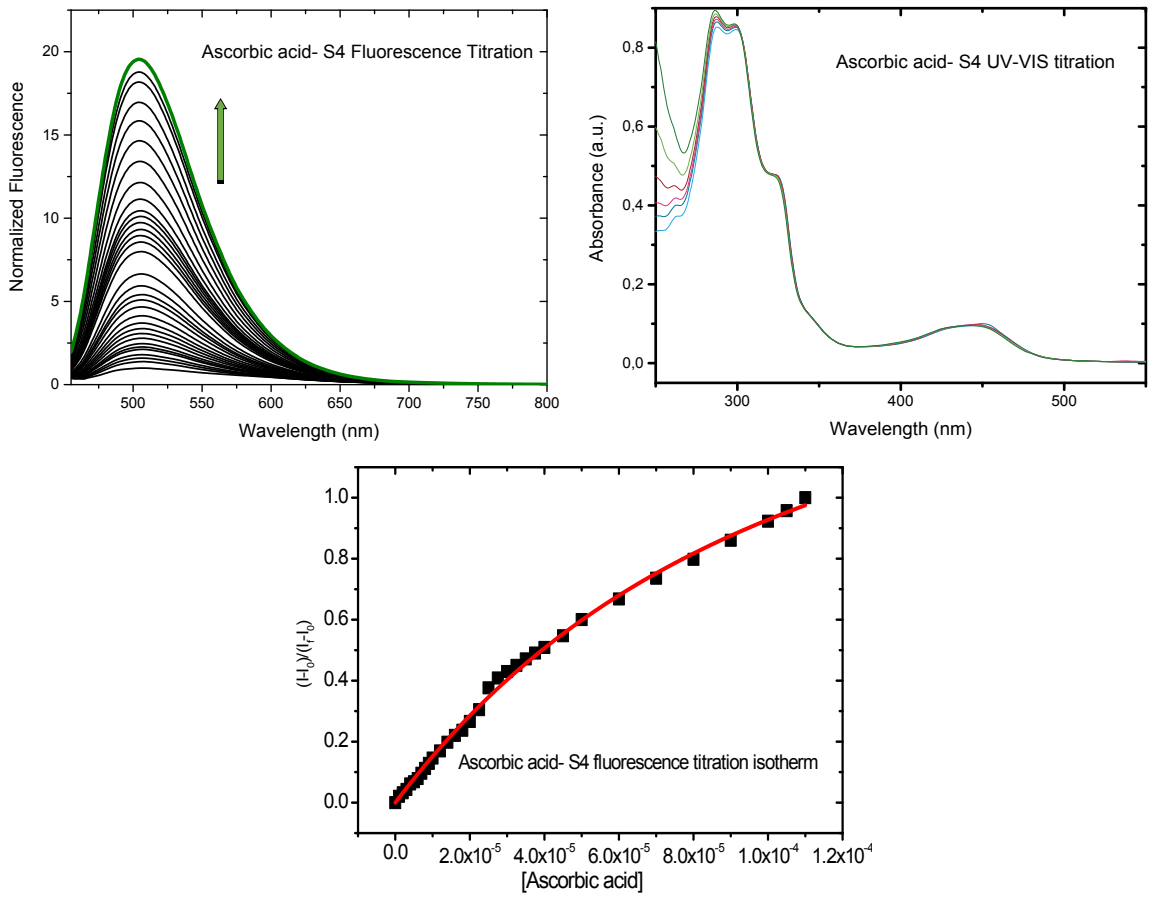

Figure S36. Fluorescence spectra (above left) and binding isotherms (bottom) of ascorbic acid– **S4** (25 µM) fluorescence titration (λexc=440) nm and UV-Vis spectra of ascorbic acid –**S4** titration (above right).

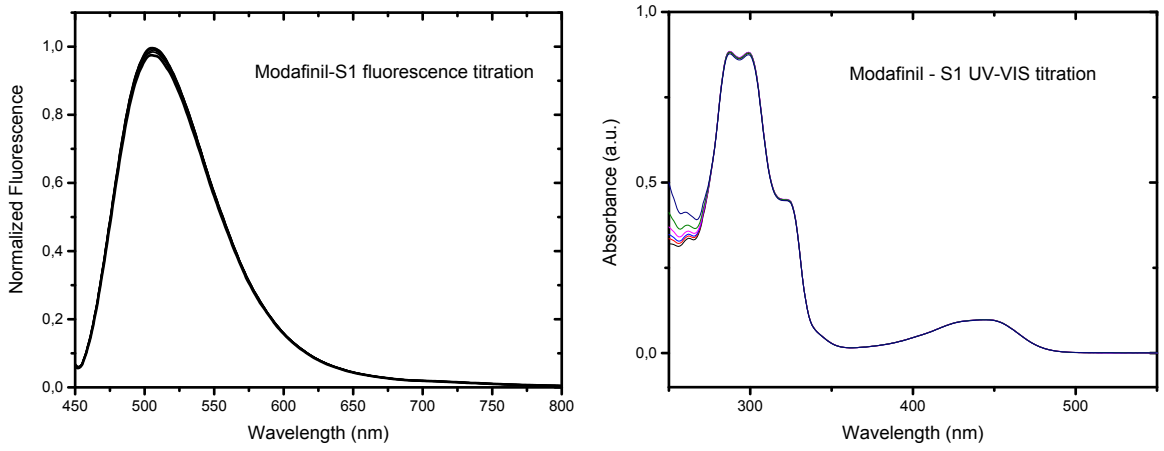

Figure S37. Fluorescence spectra (left) of modafinil– **S1** (20 µM) fluorescence titration (λ_{exc}=438 nm) and UV-Vis spectra of modafinil –**S1** titration (right).

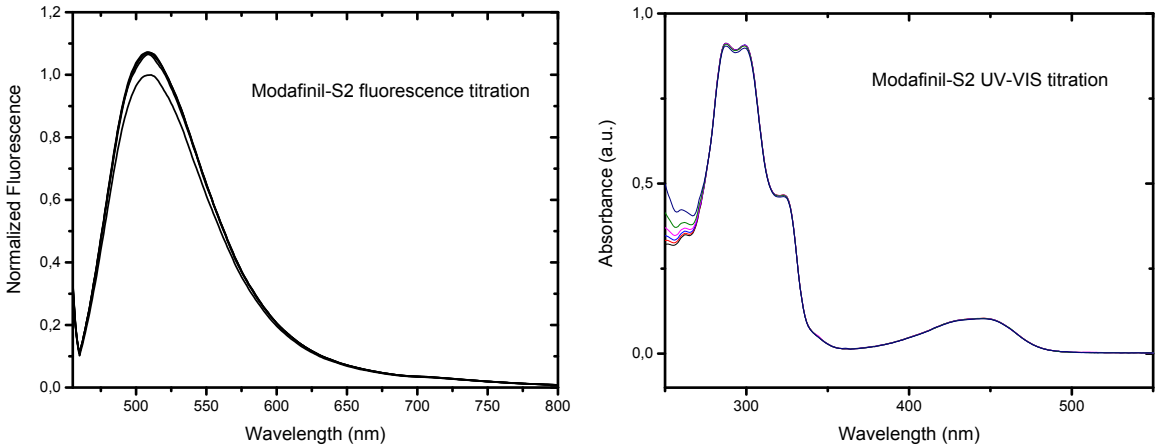

Figure S38. Fluorescence spectra (left) of modafinil– **S2** (20 µM) fluorescence titration (λ_{exc}=443 nm) and UV-Vis spectra of modafinil –**S2** titration (right).

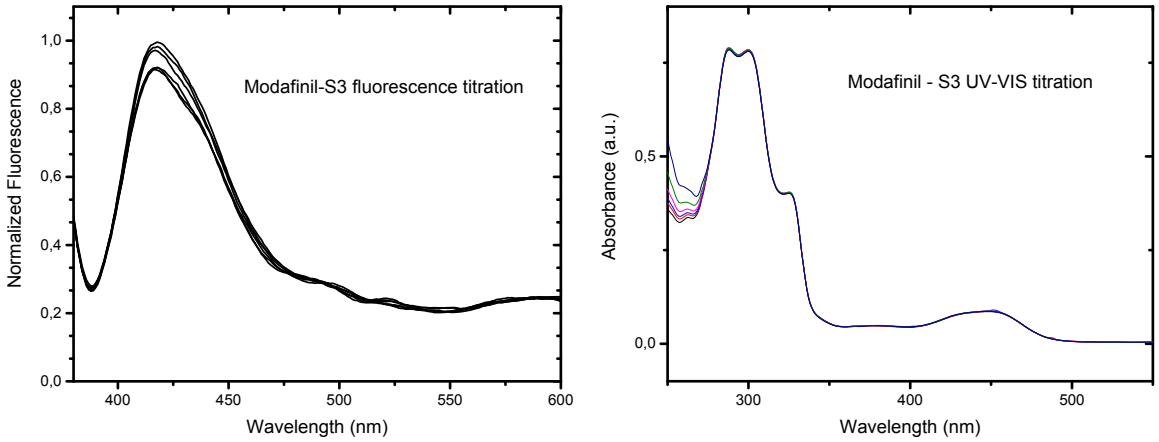

Figure S39. Fluorescence spectra (left) of modafinil– **S3** (2 µM) fluorescence titration (λ_{exc}=336 nm) and UV-Vis spectra of modafinil –**S3** titration (right).

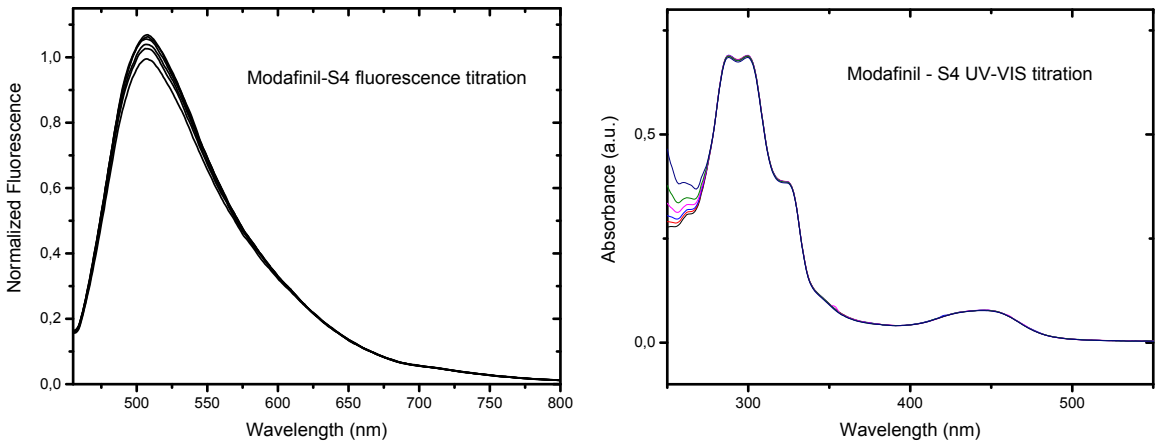

Figure S40. Fluorescence spectra (left) of modafinil– **S4** (25 µM) fluorescence titration (λ_{exc}=440 nm) and UV-Vis spectra of modafinil –**S4** titration (right).

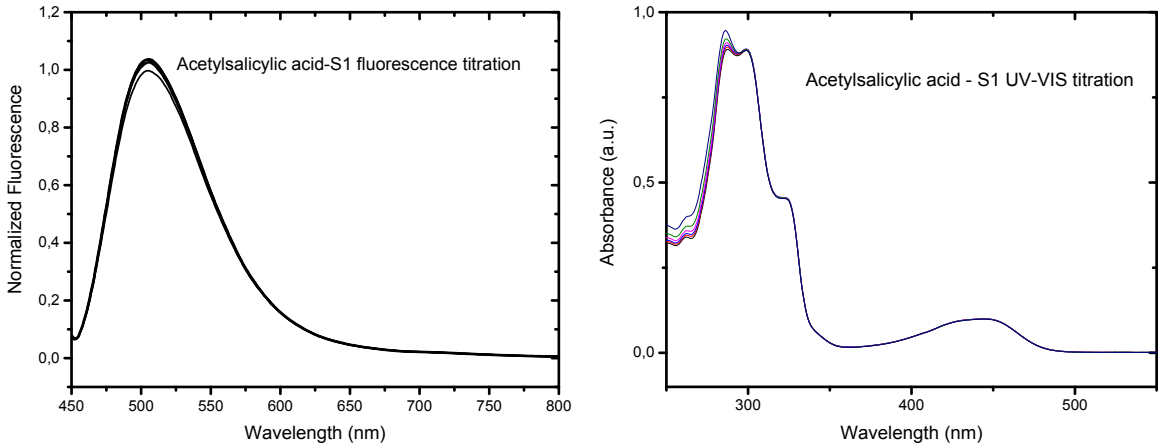

Figure S41. Fluorescence spectra (left) of acetylsalicyclic acid– **S1** (20 µM) fluorescence titration (λ_{exc}=438 nm) and UV-Vis spectra of acetylsalicyclic acid– **S1** titration (right).

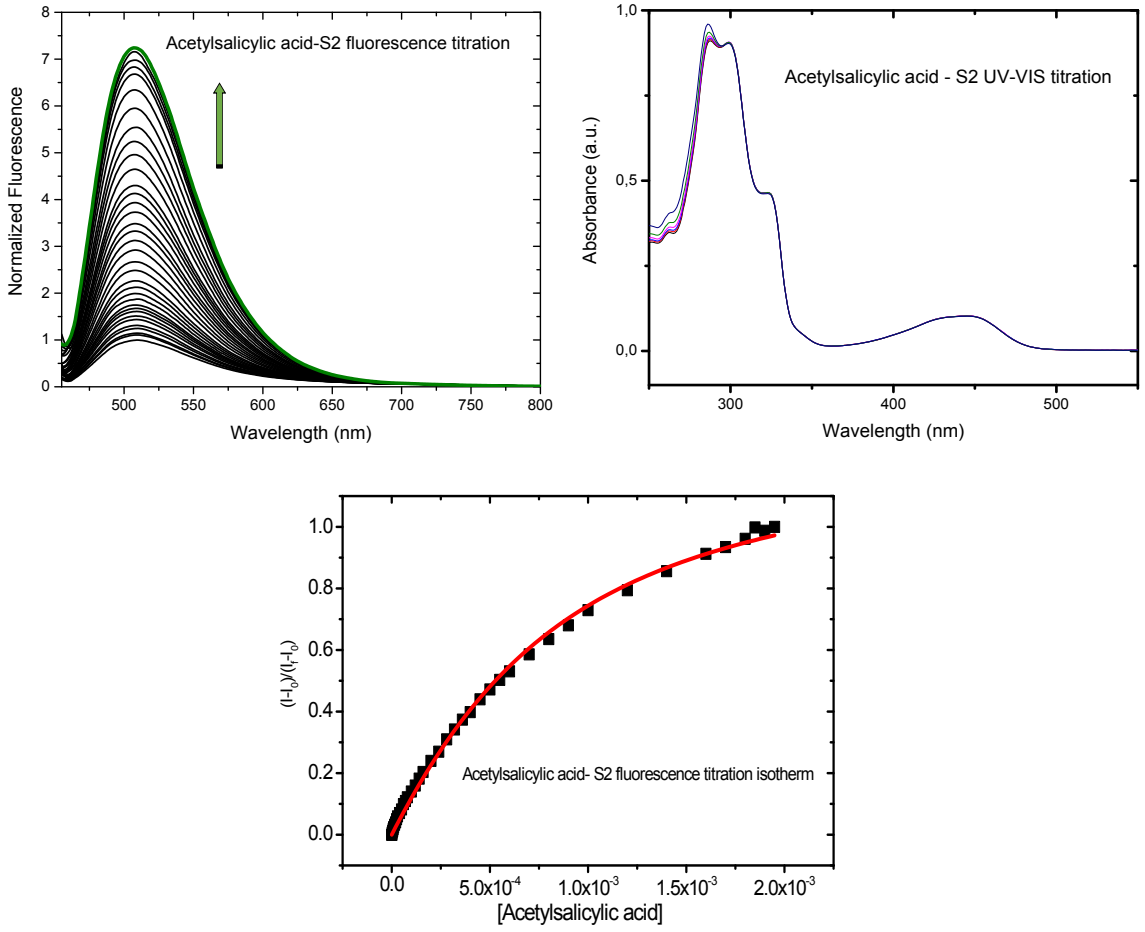

Figure S42. Fluorescence spectra (above left) and binding isotherms (bottom) of acetylsalicyclic acid – **S2** (20 µM) fluorescence titration (λexc=443) nm and UV-Vis spectra of acetylsalicyclic acid –**S2** titration (above right).

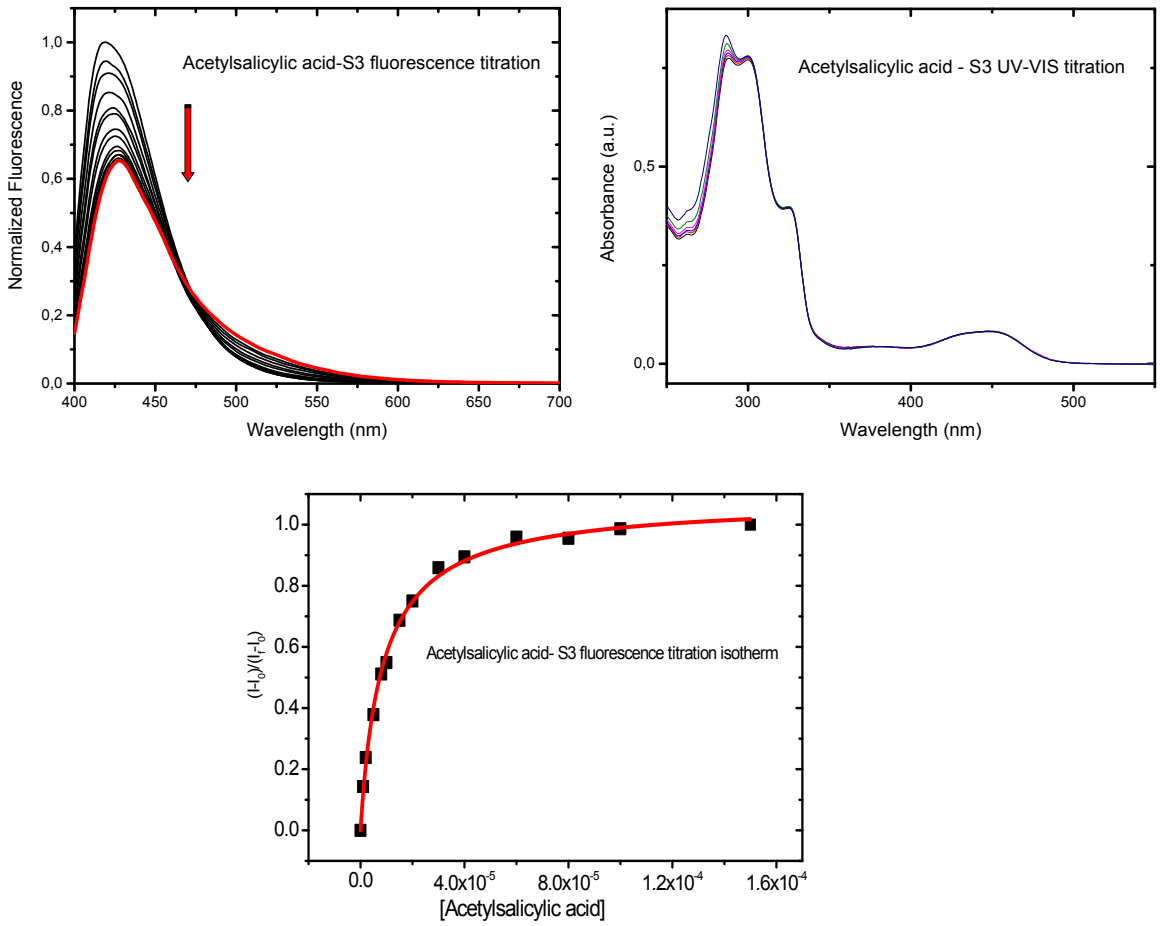

Figure S43. Fluorescence spectra (above left) and binding isotherms (bottom) of acetylsalicyclic acid – **S3** (2 μM) fluorescence titration (λexc=380) nm and UV-Vis spectra of acetylsalicyclic acid –**S3** titration (above right).

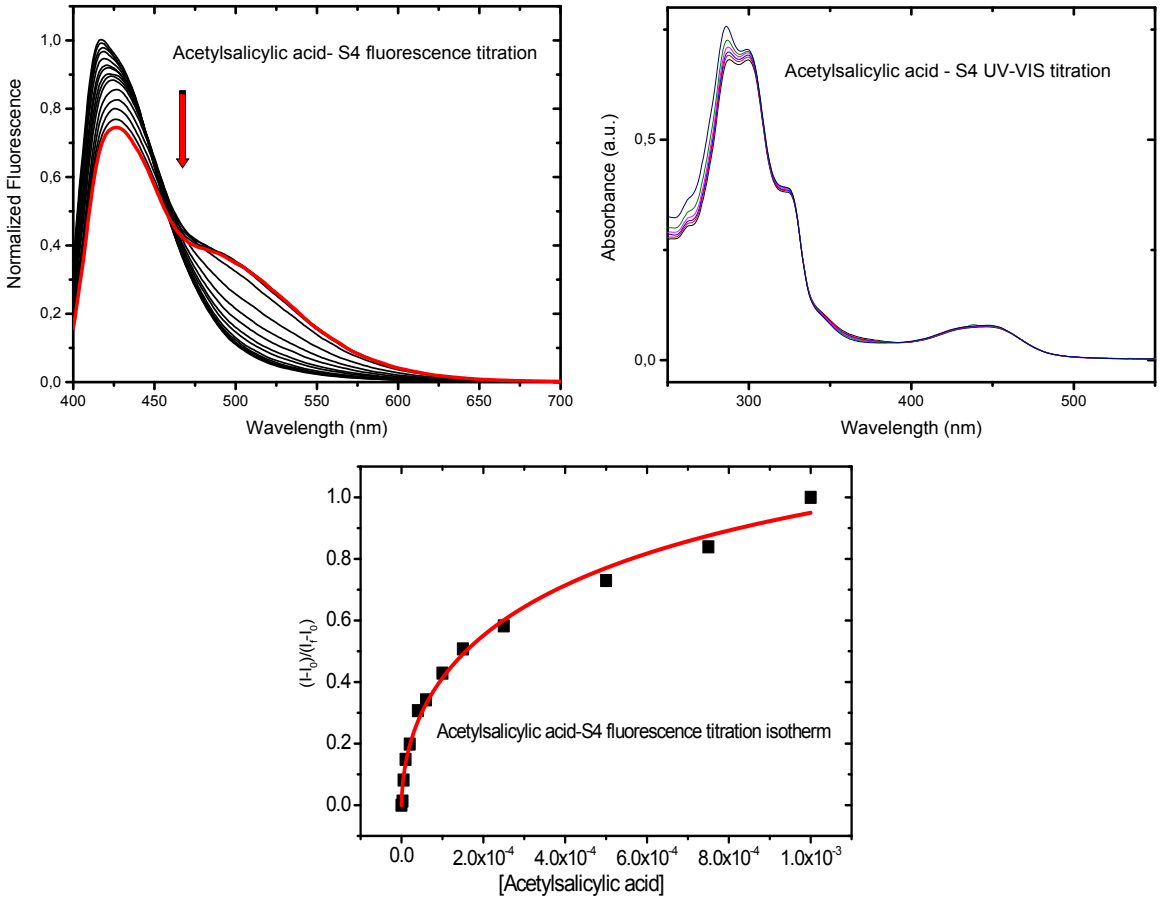

Figure S44. Fluorescence spectra (above left) and binding isotherms (bottom) of acetylsalicyclic acid – **S4** (25 μM) fluorescence titration (λexc=393) nm and UV-Vis spectra of acetylsalicyclic acid –**S4** titration (above right).

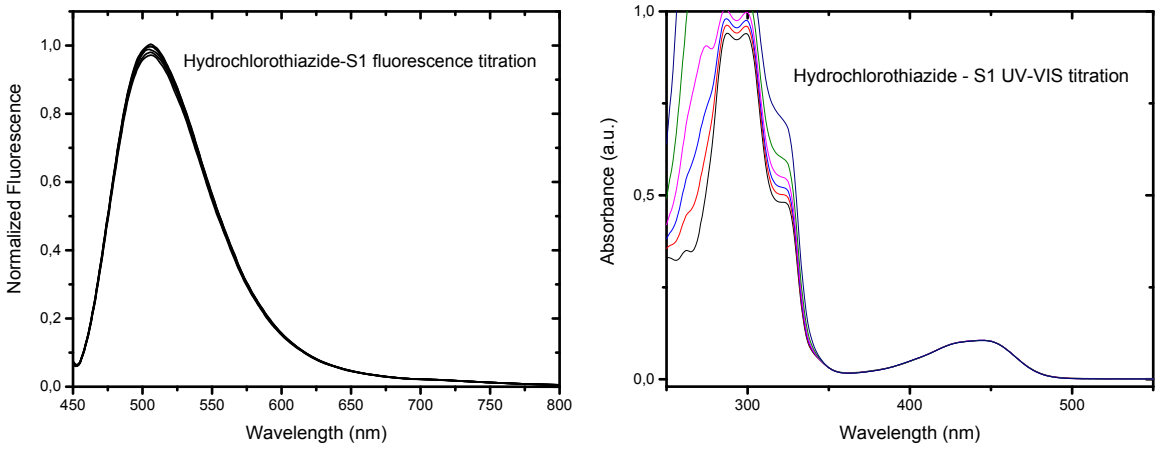

Figure S45. Fluorescence spectra (left) of hydrochlorothiazide– **S1** (20 μM) fluorescence titration (λexc=438 nm) and UV-Vis spectra of hydrochlorothiazide – **S1** titration (right).

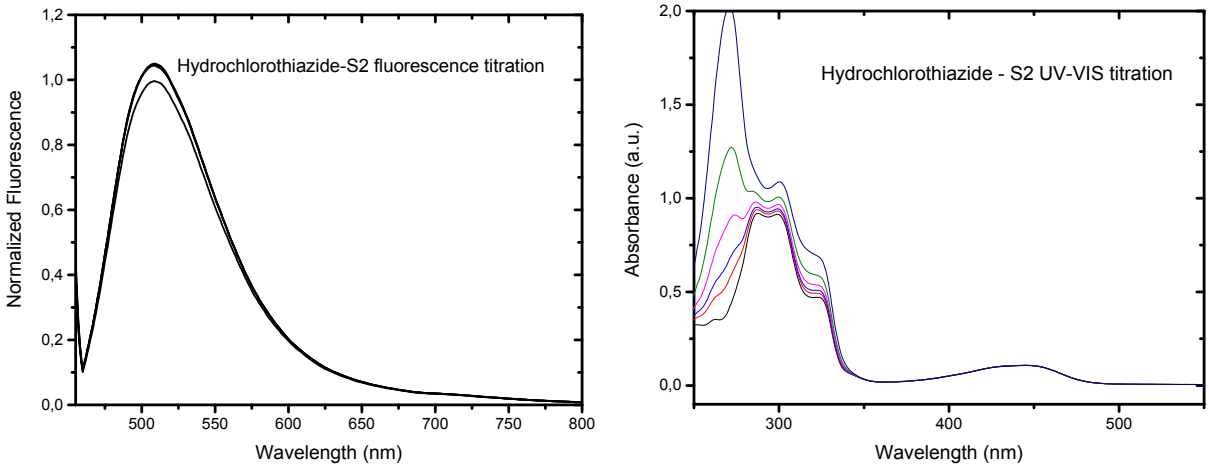

Figure S46. Fluorescence spectra (left) of hydrochlorothiazide– **S2** (20 µM) fluorescence titration (λexc=443 nm) and UV-Vis spectra of hydrochlorothiazide – **S2** titration (right).

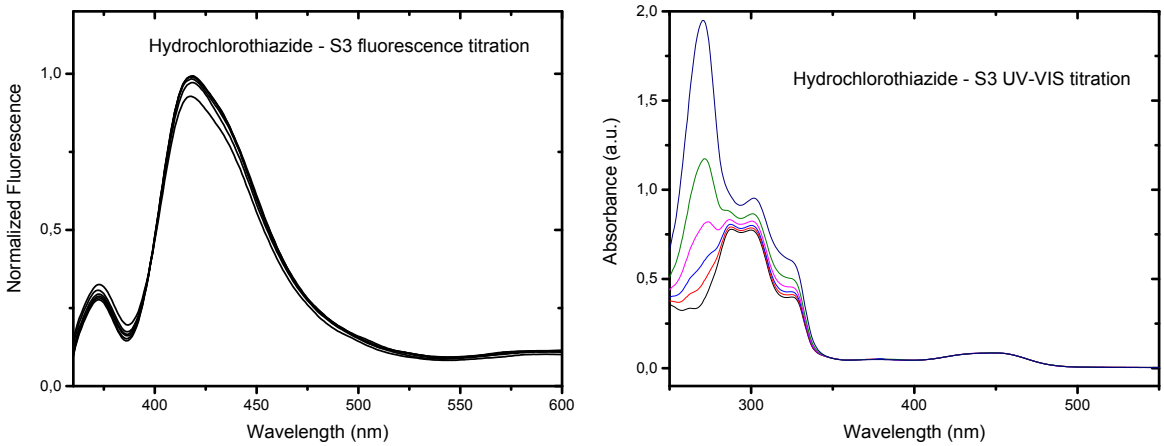

Figure S47. Fluorescence spectra (left) of hydrochlorothiazide– **S3** (2 µM) fluorescence titration (λexc=336 nm) and UV-Vis spectra of hydrochlorothiazide – **S3** titration (right).

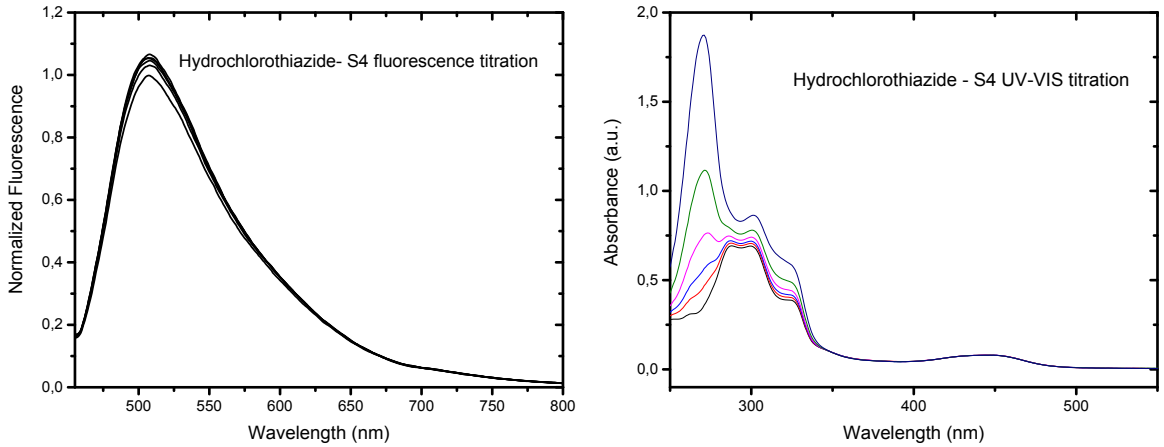

Figure S48. Fluorescence spectra (left) of hydrochlorothiazide– **S4** (25 µM) fluorescence titration (λexc=440 nm) and UV-Vis spectra of hydrochlorothiazide – **S4** titration (right).

MALDI Study

1mM solutions of S1-S4 were prepared in LC-MS grade acetonitrile and 1 mM meldonium was prepared in LC-MS grade methanol. Then meldonium was mixed with each of the sensor separately as their final concentration will be 1µM in vials. ESI and MALDI were used to get the mass spectra of non-covalent complexes but it was not possible to get any information from ESI since noncovalent complex was unstable to vaporization and ionization conditions. On the other hand, acceptable results were obtained from MALDI when dihydrobenzoic acid (DHB) was used as matrix. Most of the complex were lost during the measurement but it was possible to detect the complexes in MALDI.

Table S1 . *MALDI Results*

	Calculated	**Found**
$[S1+M+Na-H-H_2O]^+$	748.40	748.38
$[S2+M]^+$	768.49	768.51
$[S3+M+Na-H-H_2O]^+$	742.44	742.35
$[S4+M-Br]^+$	711.45	711.45

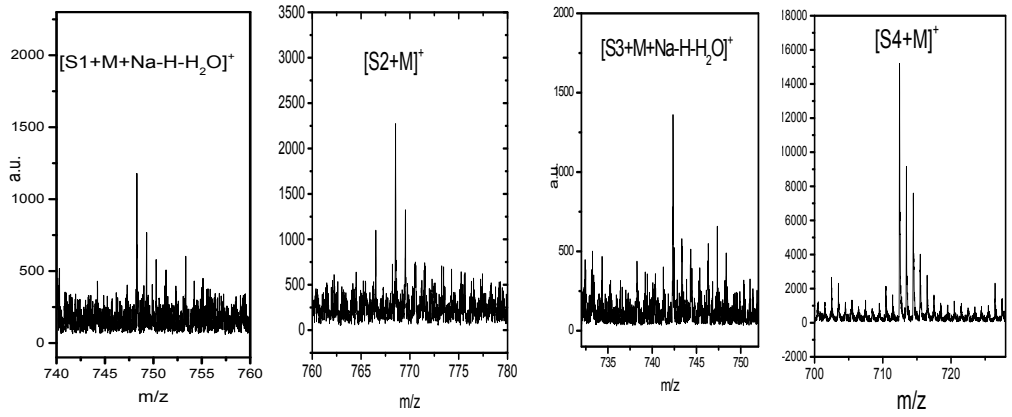

Figure S49. MALDI spectra of meldonium – chemosensor complexes

^{1}H-NMR titrations

4.3 µmol S1-S4 were dissolved in 100 µL DMSO-d6 and 400 µL acetonitrile-d3 in separate NMR vials. 34 µmol meldonium were dissolved in 500 µL methanol-d4. NMR titrations were conducted using equivalent points of sensor molecules. Upfield shifting can be clearly observed on amide band of S1-S3 but for S4 after 0.33 eq amide peak was disappeared due to low signal of amide in S4. However upfield shifting still can be observed in the first addition.

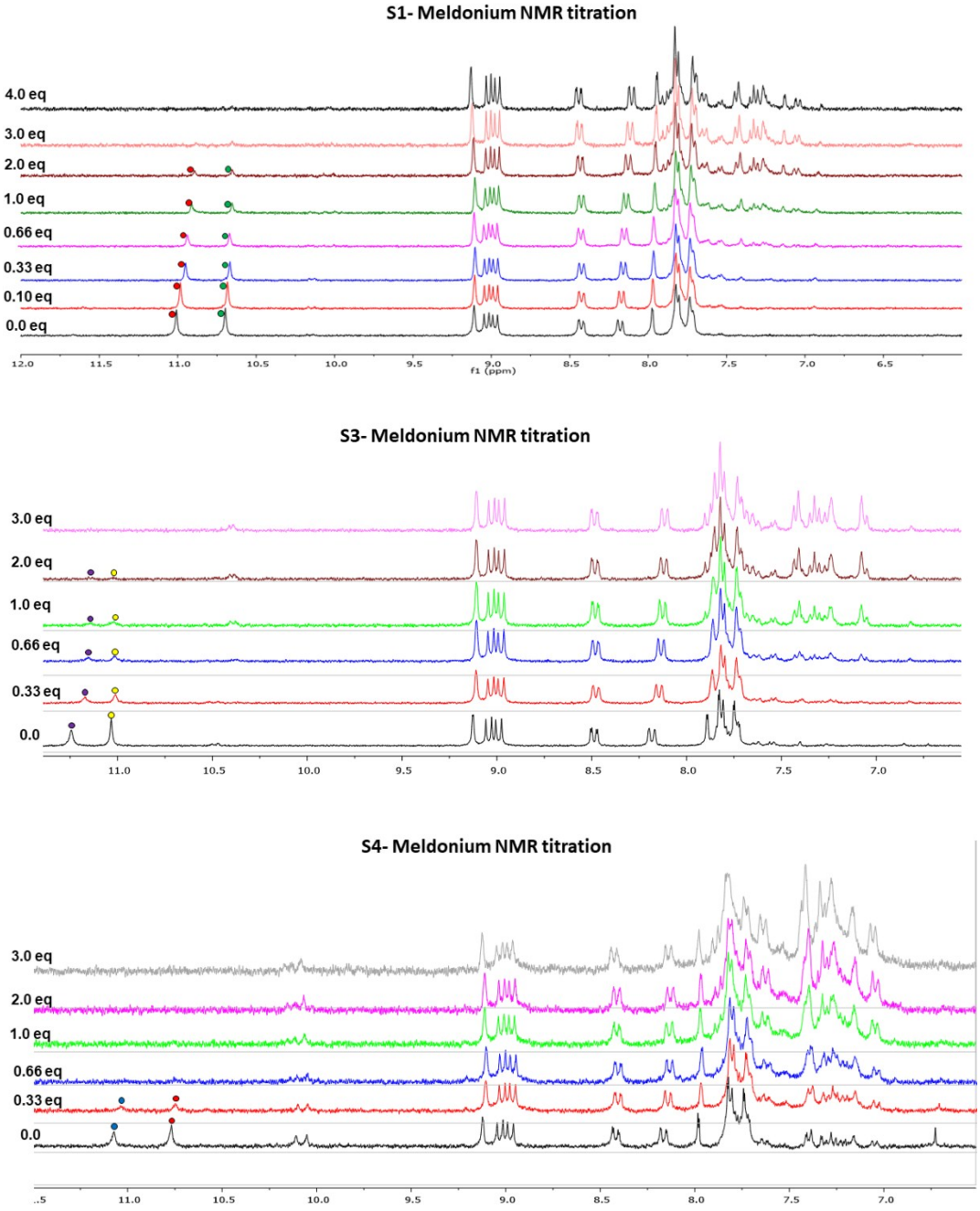

Figure S50. NMR titrations of meldonium and chemosensors

Thermodynamic parameters

Thermodynamic parameters were calculated using fluorescence titrations at four different temperatures. Binding constants at three different temperatures were calculated and van't Hoff plots for each chemosensors were plotted using 1/T and lnK values. According to equation 1, slope of Van't Hoff plots gives ΔH/R while intercepts of the m are ΔS/R. After calculation of enthalpy and entropy changes, Gibss free energy changes were calculated using equation 2.

$$\ln k = \Delta H/RT + \Delta S/R \qquad \text{(Equation 1)}$$

$$\Delta G = \Delta H - T\Delta S \qquad \text{(Equation 2)}$$

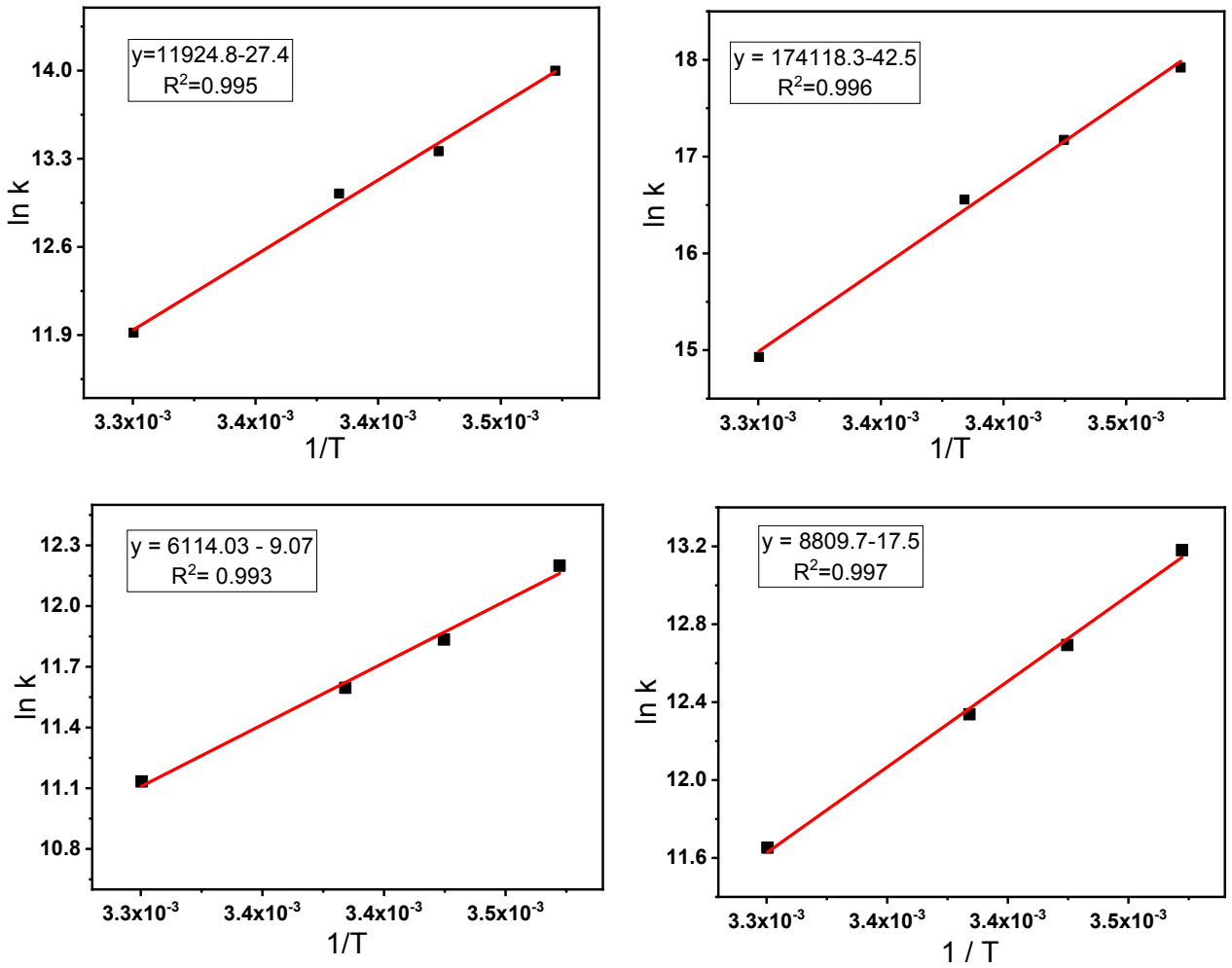

Figure S51.van't Hoff plots for meldonium and **S1**, **S2**, **S3** and **S4** fluorescence titrations

Sensor Array studies

Arrays on 96-Well plate

In qualitative analysis 40 µL of stock sensor solutions (100 µM) were pipetted in each well. Then, of each of the analytes (800 µM) were added to their lines (10 wells for each analyte) in the 96-well plate. After 30 seconds stirring in microplate reader, they were measured using end-point mode. Data were then transferred to Systat software for Linear Discriminant Analysis.

Fo rquantitative analyses, different concentration of meldonium in methanol were added to the sensors firstly. Then the data evaluated using LDA for semi-quantitative analysis. Finally the data were evaluated using Solo Chemometrics software. The lowest error values in calibration, cross-validation and prediction were acquired in ANN. After getting promising results from organic solvents meldonium was spiked to synthetic urine samples and same procedures were applied.

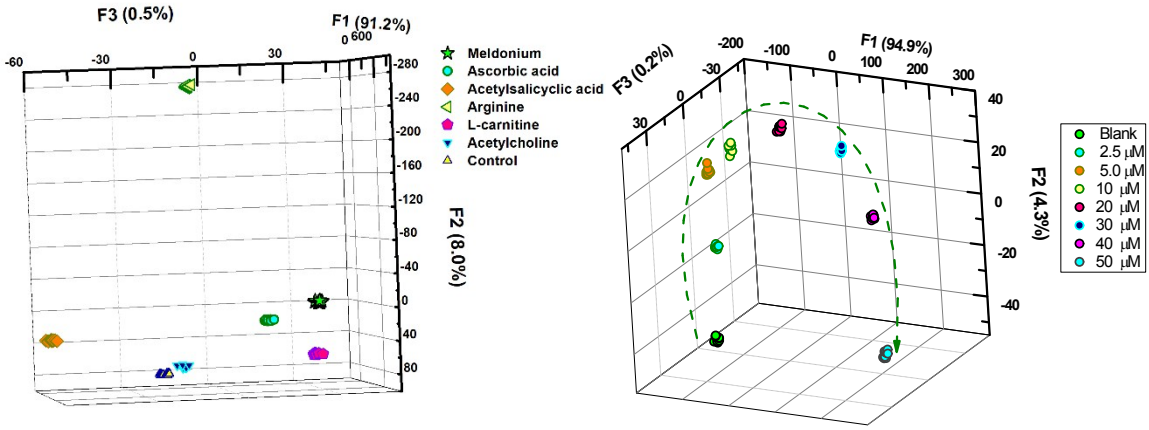

Figure S52. Analytes in organic solvents (acetonitrile and methanol): Qualitative discrimination (left) and semi-quantitative analysis (of meldonium) of the multivariate responses obtained from 96-well plate measurements in microplate reader using linear discriminant analysis

Table S2. The jackknifed classification matrix and other test statistics of qualitative LDA of analytes in organic solvents and 96-well plate measurements in microplate reader

Jackknifed Classification Matrix

	Acetylcholine	Acetylsalicyclic acid	Arginine	Ascorbic acid	Control	L-carnitine	Meldonium	%correct
Acetylcholine	10	0	0	0	0	0	0	100
Acetylsalicyclic acid	0	10	0	0	0	0	0	100
Arginine	0	0	10	0	0	0	0	100
Ascorbic acid	0	0	0	10	0	0	0	100
Control	0	0	0	0	10	0	0	100
L-carnitine	0	0	0	0	0	10	0	100
Meldonium	0	0	0	0	0	0	10	100
Total	10	10	10	10	10	10	10	100

Eigenvalues

171,955.147	15,003.658	1,018.439	509.328	61.873	11.551

Canonical Correlations

1.000	1.000	1.000	0.999	0.992	0.959

Cumulative Proportion of Total Dispersion					
0.912	0.992	0.997	1.000	1.000	1.000

Test Statistic				
Statistic	Value	Approx. F-ratio	df	p-value
Wilks's Lambda	0.000	742.486	234, 156	0.000
Pillai's Trace	5.901	46.044	234, 180	0.000
Lawley-Hotelling Trace	188,559.996	18,802.279	234, 140	0.000

Canonical Scores Plot

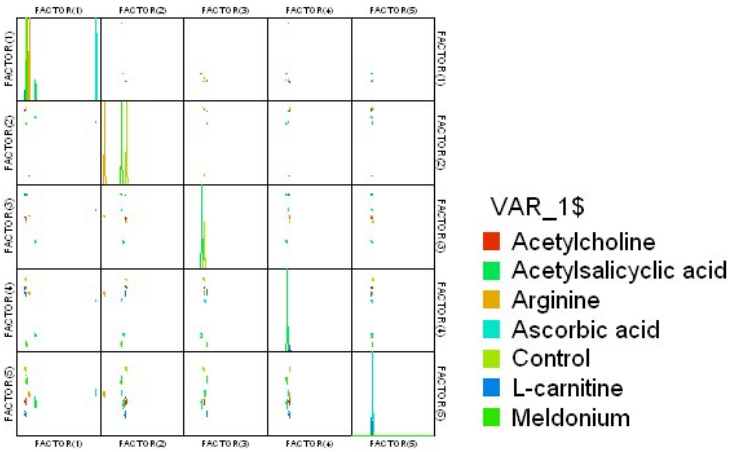

Table S3. The jackknifed classification matrix and other test statistics of semi-quantitative LDA of analytes in organic solvents and 96-well plate measurements in microplate reader

Jackknifed Classification Matrix									
	0	2.5	5	10	20	30	40	50	%correct
0	10	0	0	0	0	0	0	0	100
2.5	0	10	0	0	0	0	0	0	100
5	0	0	10	0	0	0	0	0	100
10	0	0	0	10	0	0	0	0	100
20	0	0	0	0	10	0	0	0	100
30	0	0	0	0	0	10	0	0	100
40	0	0	0	0	0	0	10	0	100
50	0	0	0	0	0	0	0	10	100
Total	10	10	10	10	10	10	10	10	100

Eigenvalues						
24,614.556	1,105.899	95.848	54.791	36.991	16.935	4.316

Canonical Correlations						
1.000	1.000	0.995	0.991	0.987	0.972	0.901

Cumulative Proportion of Total Dispersion						
0.949	0.992	0.996	0.998	0.999	1.000	1.000

Test Statistic				
Statistic	Value	Approx. F-ratio	df	p-value
Wilks's Lambda	0.000	90.186	315, 203	0.000
Pillai's Trace	6.701	16.911	315, 238	0.000

Test Statistic				
Statistic	**Value**	**Approx. F-ratio**	**df**	**p-value**
Lawley-Hotelling Trace	25,929.337	2,163.718	315, 184	0.000

Canonical Scores Plot

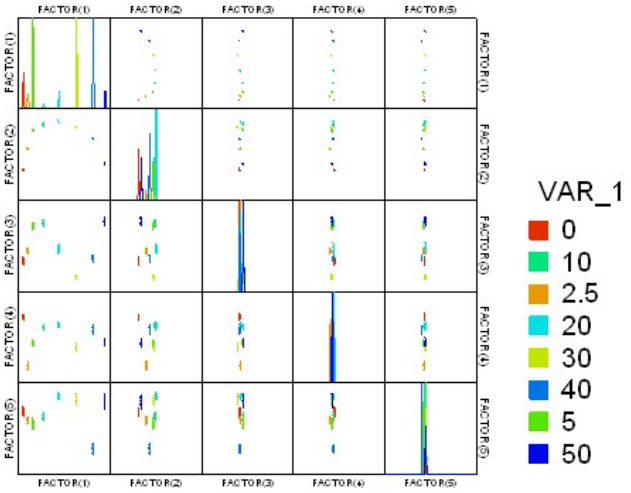

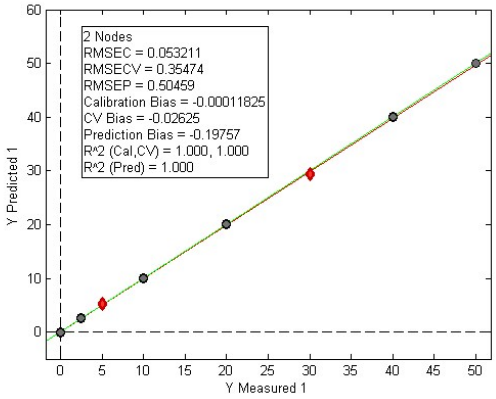

Figure S53. Artificial Neural Network Analysis for quantitation of meldonium in methanol

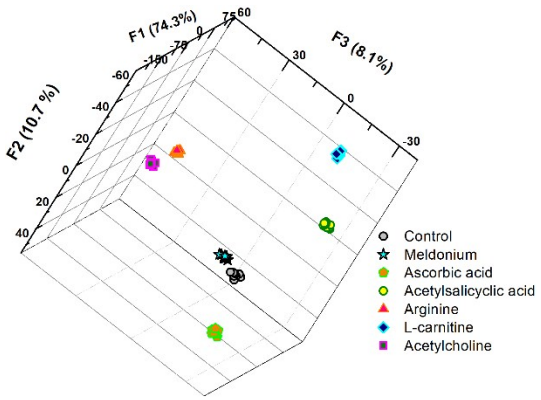

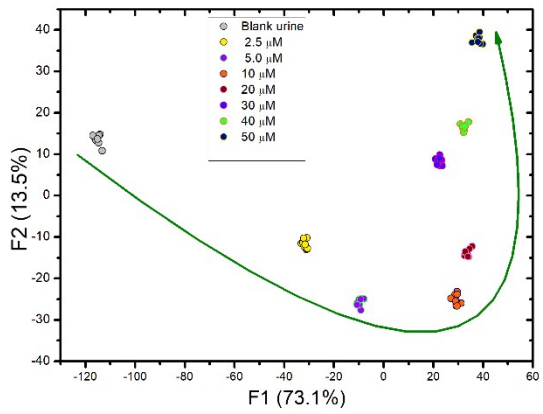

Figure S54. Analytes in urine: Qualitative discrimination (left) and semi-quantitative analysis (of meldonium) of the multivariate responses obtained from 96-well plate measurements in microplate reader using linear discriminant analysis

Table S4. The jackknifed classification matrix and other test statistics of qualitative LDA of analytes in urine and 96-well plate measurements in microplate reader

Jackknifed Classification Matrix

	Acetylcholine	Acetylsalicyclic acid	Arginine	Ascorbic acid	Control	L-carnitine	Meldonium	%correct
Acetylcholine	10	0	0	0	0	0	0	100
Acetylsalicyclic acid	0	10	0	0	0	0	0	100
Arginine	0	0	10	0	0	0	0	100
Ascorbic acid	0	0	0	10	0	0	0	100
Control	0	0	0	0	10	0	0	100
L-carnitine	0	0	0	0	0	10	0	100
Meldonium	0	0	0	0	0	0	10	100
Total	10	10	10	10	10	10	10	100

Eigenvalues

7.499,969	1.080,335	812,959	354,503	281,993	60,947

Canonical Correlations

1,000	1,000	0,999	0,999	0,998	0,992

Cumulative Proportion of Total Dispersion

0,743	0,850	0,931	0,966	0,994	1,000

Test Statistic

Statistic	Value	Approx. F-ratio	df		p-value
Wilks's Lambda	0,000	118,338	330	60	0,000
Pillai's Trace	5,975	61,389	330	84	0,000
Lawley-Hotelling Trace	10.090,708	224,238	330	44	0,000

Canonical Scores Plot

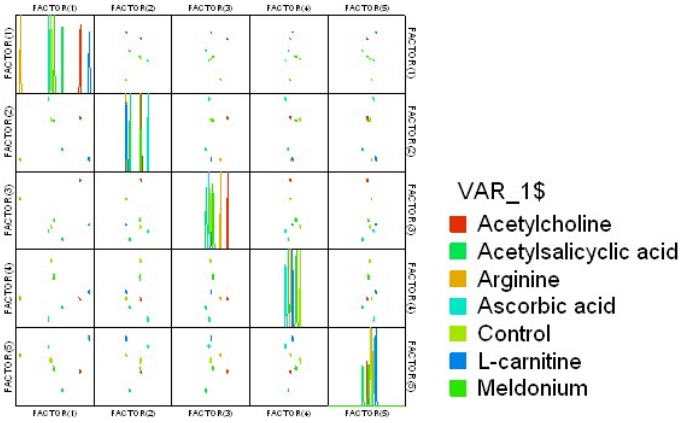

Table S5. The jackknifed classification matrix and other test statistics of semi-quantitative LDA of analytes in urine and 96-well plate measurements in microplate reader

Jackknifed Classification Matrix

	0	2.5	5	10	20	30	40	50	%correct
0	10	0	0	0	0	0	0	0	100
2.5	0	10	0	0	0	0	0	0	100
5	0	0	10	0	0	0	0	0	100
10	0	0	0	10	0	0	0	0	100
20	0	0	0	0	10	0	0	0	100
30	0	0	0	0	0	10	0	0	100
40	0	0	0	0	0	0	10	0	100
50	0	0	0	0	0	0	0	10	100
Total	10	10	10	10	10	10	10	10	100

Eigenvalues

2.683,878	495,254	208,962	155,897	85,517	23,000	18,179

Canonical Correlations

1,000	0,999	0,998	0,997	0,994	0,979	0,974

Cumulative Proportion of Total Dispersion

0,731	0,866	0,923	0,965	0,989	0,995	1,000

Test Statistic

Statistic	Value	Approx. F-ratio	df		p-value
Wilks's Lambda	0,000	52,488	392	130	0,000
Pillai's Trace	6,881	23,771	392	161	0,000
Lawley-Hotelling Trace	3.670,687	143,135	392	107	0,000

Canonical Scores Plot

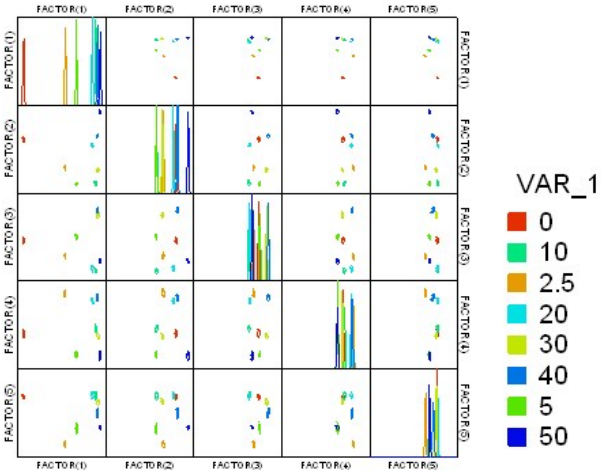

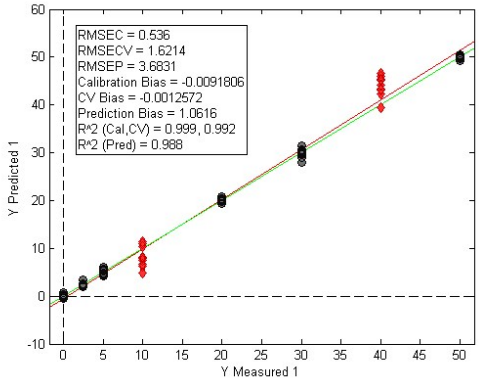

Figure S55. Artificial Neural Network Analysis for quantitation of meldonium in urine using 96-well plate and microplate reader

Paper Microzone Plates Measured with Simple Instrumentation

Experimental details were given in the experimental section of the main text. The printed paper microzone plates can be seen in Figure S25 . Only qualitative analysis was achieved in these experiments.

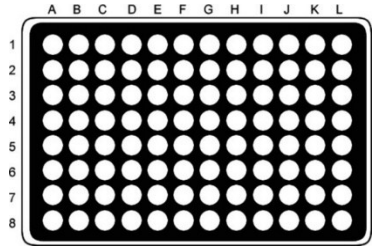

Figure S56: Paper microzone plate

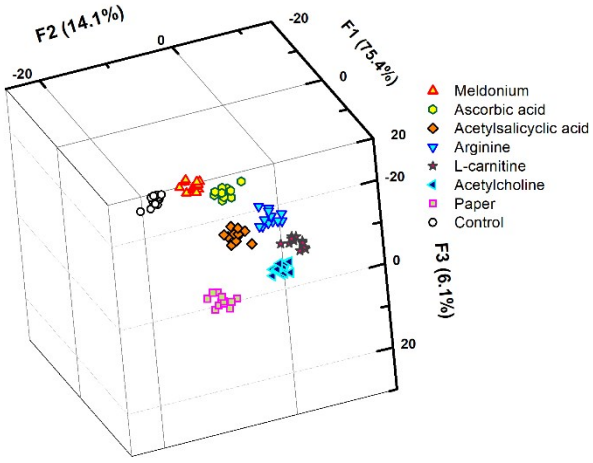

Figure S57. Analytes in urine. Qualitative discrimination of the multivariate responses (LDA score plot) obtained from paper microzone plates measurements using a UV-lamp, optical filters and a mobile phone

Table S6. The jackknifed classification matrix and other test statistics of qualitative LDA of analytes in urine and paper microzone plates measurements using a UV-lamp, optical filters and a mobile phone

Jackknifed Classification Matrix

	Acetylcholine	Acetylsalicyclic acid	Arginine	Ascorbic acid	Control	L-carnitine	Meldonium	Paper	%correct
Acetylcholine	12	0	0	0	0	0	0	0	100
Acetylsalicyclic acid	0	12	0	0	0	0	0	0	100
Arginine	0	0	12	0	0	0	0	0	100
Ascorbic acid	0	0	0	12	0	0	0	0	100
Control	0	0	0	0	12	0	0	0	100
L-carnitine	0	0	0	0	0	12	0	0	100
Meldonium	0	0	0	0	0	0	12	0	100
Paper	0	0	0	0	0	0	0	12	100
Total	12	12	12	12	12	12	12	12	100

Eigenvalues

144.777	27.080	11.746	4.332	2.781	0.897	0.416

Canonical Correlations

0.997	0.982	0.960	0.901	0.858	0.688	0.542

Cumulative Proportion of Total Dispersion

0.754	0.895	0.956	0.979	0.993	0.998	1.000

Test Statistic

Statistic	Value	Approx. F-ratio	df		p-value
Wilks's Lambda	0.000	17.219	196	425	0.000
Pillai's Trace	5.194	6.880	196	469	0.000
Lawley-Hotelling Trace	192.030	58.085	196	415	0.000

Canonical Discriminant Functions

	1	2	3	4	5	6	7
Constant	38.184	9.336	28.065	-15.255	32.334	-6.938	-16.058

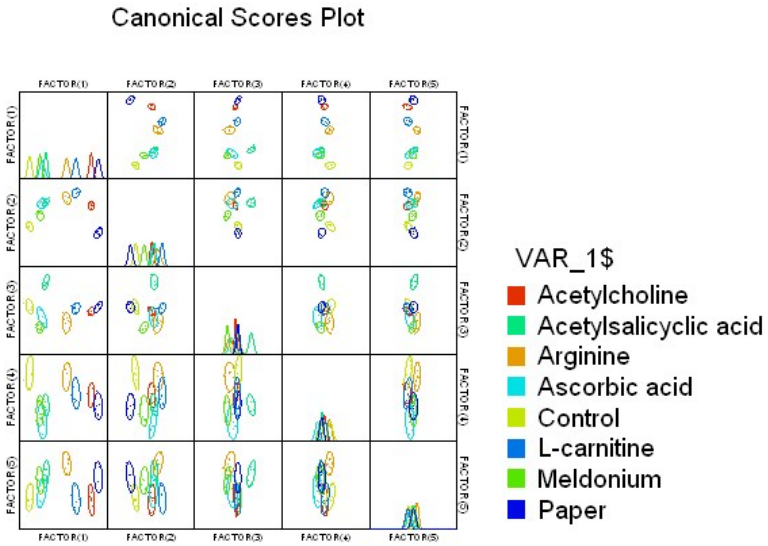

Paper Microzone Plates Measured with Microplate Reader

Experimental details were given in the main text. Qualitative and semi-quantitative analysis were done by LDA while quantitative analysis of meldonium in urine was achieved using ANN regression.

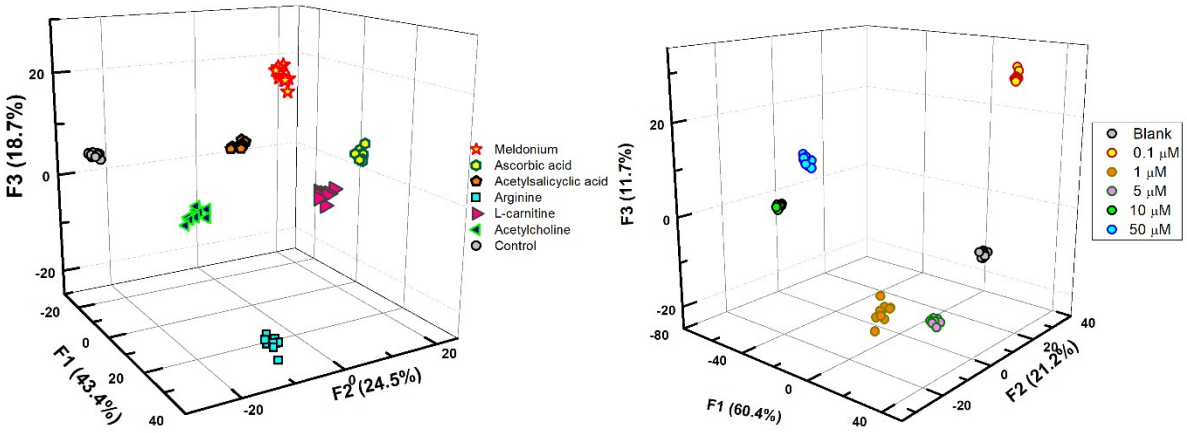

Figure S58. Analytes in urine: Qualitative discrimination (left) and semi-quantitative analysis (of meldonium) of the multivariate responses obtained from paper microzone plates measured in microplate reader using linear discriminant analysis

Table S7. The jackknifed classification matrix and other test statistics of qualitative LDA of analytes in urine and paper microzone plates measured in microplate reader

Jackknifed Classification Matrix

	Acetylcholine	Acetylsalicyclic acid	Arginine	Ascorbic acid	Control	L-carnitine	Meldonium	%correct
Acetylcholine	10	0	0	0	0	0	0	100
Acetylsalicyclic acid	0	10	0	0	0	0	0	100
Arginine	0	0	10	0	0	0	0	100
Ascorbic acid	0	0	0	10	0	0	0	100
Control	0	0	0	0	10	0	0	100
L-carnitine	0	0	0	0	0	10	0	100
Meldonium	0	0	0	0	0	0	10	100
Total	10	10	10	10	10	10	10	100

Eigenvalues

453,400	256,227	192,247	76,778	45,939	20,716

Canonical Correlations

0,999	0,998	0,997	0,994	0,989	0,977

Cumulative Proportion of Total Dispersion

0,434	0,679	0,863	0,936	0,980	1,000

Test Statistic

Statistic	Value	Approx. F-ratio	df		p-value
Wilks's Lambda	0,000	48,426	276	114	0,000
Pillai's Trace	5,909	32,296	276	138	0,000
Lawley-Hotelling Trace	1.045,307	61,860	276	98	0,000

Canonical Discriminant Functions

	1	2	3	4	5	6
Constant	-98,395	34,416	-45,895	-23,593	-0,678	-14,900

Canonical Scores Plot

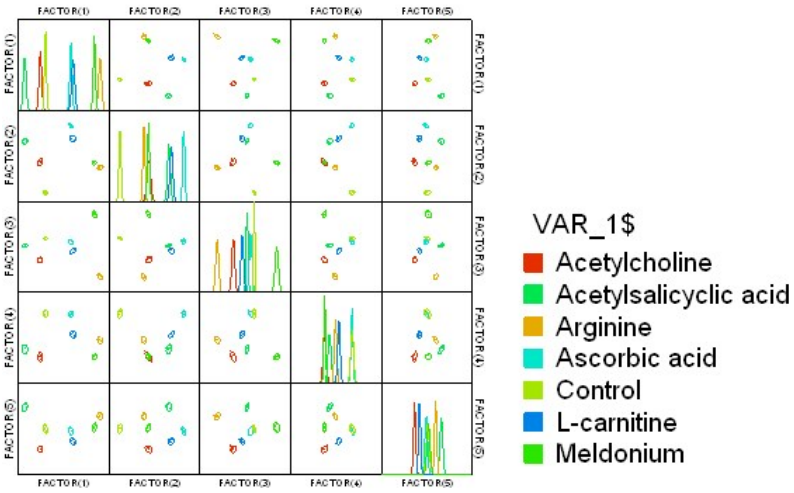

Table S8. The jackknifed classification matrix and other test statistics of semi-quantitative LDA of analytes in urine and paper microzone plates measured in microplate reader

Jackknifed Classification Matrix

	0	0.1	1	5	10	50	%correct
0	10	0	0	0	0	0	100
0.1	0	10	0	0	0	0	100
1	0	0	10	0	0	0	100
5	0	0	0	10	0	0	100
10	0	0	0	0	10	0	100
50	0	0	0	0	0	10	100
Total	10	10	10	10	10	10	100

Eigenvalues

1.641,415	573,254	317,550	141,326	41,916

Canonical Correlations

1,000	0,999	0,998	0,996	0,988

Cumulative Proportion of Total Dispersion

0,604	0,816	0,933	0,985	1,000

Test Statistic

Statistic	Value	Approx. F-ratio	df		p-value
Wilks's Lambda	0,000	57,740	235	42	0,000
Pillai's Trace	4,964	35,387	235	60	0,000
Lawley-Hotelling Trace	2.715,461	73,953	235	32	0,000

Canonical Discriminant Functions

	1	2	3	4	5
Constant	225,145	40,003	-21,931	14,677	-28,198

Canonical Scores Plot

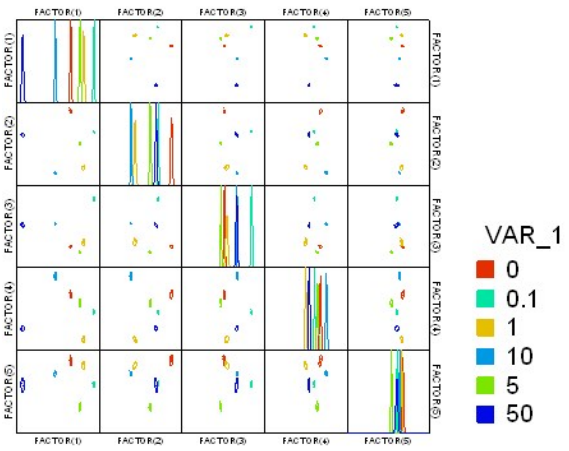

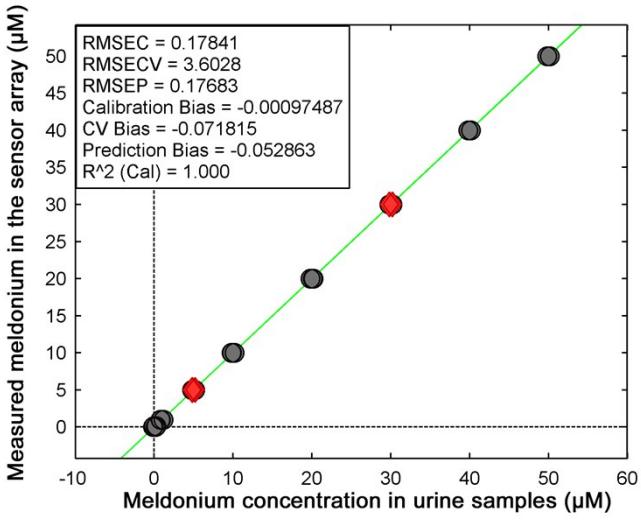

Figure S59. Support Vector Machine Analysis for quantitation of meldonium in urine using paper microzone plate and microplate reader

Comparison of Analytical Performances

Table S2 . *Comparison of analytical methods in terms of time, sensitivity, range and application*

Method	Retention time (min)	Linear range (µg mL^{-1})	LOD (ng mL^{-1})	Applications	Reference
LC–MS/MS[a]	6.20	0.01-0.25	7.5	Urine	[8]
Electrochemical method	-	0.1–5.0	66	Urine	[9]
LC–MS/MS [a]	7.26	0.001–0.02	1.0	Human plasma and urine	[10]
LC–MS/MS [a]	4.1	0.01–20	-	Human plasma	[11]
CE[b]	2.81	0.02–4.0 and 2–200	15	Urine	[12]
HRMS[c]	0.48	0.05 – 2.0	~50	Urine	[13]
UPLC-MS/MS[d]	2.71	0.10 -100.00	~33	Human plasma	[14]
		0.50 - 600.00	~167	Urine	
Fluorescence sensing	HTS[e]	0.014 – 7.3	1.6	Synthetic urine	[This work]

[a]: liquid chromatography–tandem mass spectrometry, [b]: Capillary electrophoresis, [c]: high-resolution mass spectrometry, [d]: ultra performance liquid chromatography–tandem mass spectrometry, [e] High-throughput screening